murine collagen-induced arthritis: protective effect of interleukin-4 and interleukin-10 treatment on cartilage destruction. Arthritis Rheum 1997;40:249–60.
41. Williams RO, Feldmann M, Maini RN. Anti-tumor necrosis factor ameliorates joint diseases in murine collagen-induced arthritis. Proc Natl Acad Sci U S A 1992;89:9784–8.
42. Brackertz D, Mitchell GF, Mackay IR. Antigen-induced arthritis in mice. I. Induction of arthritis in various strains of mice. Arthritis Rheum 1977;20:841–50.
43. Hietala MA, Jonsson IM, Tarkowski A, Kleinau S, Pekna M. Complement deficiency ameliorates collagen-induced arthritis in mice. J Immunol 2002;169:454–9.
44. Baeten D, Boots AM, Steenbakkers PG, Elewaut D, Bos E, Verheijden GF, et al. Human cartilage gp-39+,CD16+ monocytes in peripheral blood and synovium: correlation with joint destruction in rheumatoid arthritis. Arthritis Rheum 2000;6:1233–43.
45. Glant TT, Cs-Szabo G, Nagase H, Jacobs JJ, Mikecz K. Progressive polyarthritis induced in BALB/c mice by aggrecan from normal and osteoarthritic human cartilage. Arthritis Rheum 1998; 41:1007–18.
46. Guerassimov A, Zhang Y, Banerjee S, Cartman A, Leroux JY, Rosenberg LC, et al. Cellular immunity to the G1 domain of cartilage proteoglycan aggrecan is enhanced in patients with rheumatoid arthritis but only after removal of keratan sulfate. Arthritis Rheum 1998;41:1019–25.
47. Leroux JY, Guerassimov A, Cartman A, Delaunay N, Webber C, Rosenberg LC, et al. Immunity to the G1 globular domain of the cartilage proteoglycan aggrecan can induce inflammatory erosive polyarthritis and spondylitis in BALB/c mice but immunity to G1 is inhibited by covalently bound keratan sulfate in vitro and in vivo. J Clin Invest 1996;97:621–32.
48. Zhang Y, Guerassimov A, Leroux JY, Cartman A, Webber C, Lalic R, et al. Arthritis induced by proteoglycan aggrecan G1 domain in BALB/c mice: evidence for T cell involvement and the immunosuppressive influence of keratan sulfate on recognition of T and B cell epitopes. J Clin Invest 1998;101:1678–86.
49. Hansson AS, Heinegard D, Holmdahl R. A new animal model for relapsing polychondritis, induced by cartilage matrix protein (matrilin-1). J Clin Invest 1999;104:589–98.
50. Blass S, Schumann F, Hain NA, Engel JM, Stuhlmuller B, Burmester GR. p205 is a major target of autoreactive T cells in rheumatoid arthritis. Arthritis Rheum 1999;42:971–80.
51. Lehmann PV, Forsthuber T, Miller A, Sercarz EE. Spreading of T cell autoimmunity to cryptic determinants of an autoantigen. Nature 1992;358:155-7.
52. McRae BL, Vanderlugt CL, DalCanto MC, Miller SD. Functional evidence for epitope spreading in the relapsing pathology of experimental autoimmune encephalomyelitis. J Exp Med 1995; 182:75–85.
53. Tuohy VK, Yu M, Yin L, Kawczak JA, Johnson JM, Mathisen PM, et al. The epitope spreading cascade during progression of experimental autoimmune encephalomyelitis and multiple sclerosis. Immunol Rev 1998;164:93–100.
54. Azizan A, Gaw JU, Govindraj P, Tapp H, Neame PJ. Chondromodulin I and pleiotrophin gene expression in bovine cartilage and epiphysis. Matrix Biol 2000;19:521–31.

International Immunology, Vol. 16, No. 1, pp. 131–138
doi: 10.1093/intimm/dxh016

T cells accumulating in the inflamed joints of a spontaneous murine model of rheumatoid arthritis become restricted to common clonotypes during disease progression

Yukage Kobari[1], Yoshikata Misaki[1], Keigo Setoguchi[1], Wenming Zhao[1], Yoshinori Komagata[1], Kimito Kawahata[1], Yoichiro Iwakura[2] and Kazuhiko Yamamoto[1]

[1]Department of Allergy and Rheumatology, University of Tokyo Graduate School of Medicine, 7-3-1 Hongo, Bunkyo-ku, Tokyo 113-8655, Japan
[2]Center for Experimental Medicine, Institute of Medical Science, University of Tokyo, Tokyo 108-8639, Japan

Keywords: autoantigen, autoimmunity, clonal expansion, rheumatoid arthritis, TCR, transgenic mouse

Abstract

Although a number of studies have revealed that T cells expand clonally in the joints of patients suffering from rheumatoid arthritis (RA), the kinetics of T cell clonality in multiple joints of an individual throughout progression of the disease is not known. By employing a TCR β chain gene-specific RT-PCR and subsequent single-strand conformation polymorphism, which enables us to monitor T cell clonality, we analyzed transgenic mice (Tg) carrying the human T cell leukemia virus type I env-pX region. These mice spontaneously develop destructive progressive arthritis similar to RA as they age. In the early stage, the majority of accumulating T cell clones differed in each of four affected feet analyzed. However, in the advanced stage, many of the clones were common to all four feet. The total number of distinct clones gradually decreased as the disease progressed. When splenocytes from arthritic elder Tg were adoptively transferred into either nude mice or young Tg, the clones common to all four feet of the donor were detected again in four feet of the recipients. These findings suggest that, as arthritis progresses, the T cell clones accumulating in the arthritic joints are gradually restricted to certain common clonotypes, some of which are arthrotropic.

Introduction

Rheumatoid arthritis (RA) is a chronic inflammatory disease characterized by persistent inflammation of synovium, destruction of cartilage and bone, and systemic illness. Based on the association with particular HLA alleles (1–3), massive infiltration of T cells into the synovial tissues (4) and T cell oligoclonal expansion in the joints (5), T cells have been proposed to play an important role in RA pathogenesis: T cells would initiate or be involved in the inflammatory process by recognizing some antigens and producing cytokines (5,6), although this viewpoint has been controversial (7).

We and others have demonstrated that T cells expand clonally in the synovium as well as the synovial fluid of RA patients (5,8–14). Furthermore, some clones were found to be common in multiple joints of the same patient (14). These findings suggest that the oligoclonally accumulated common T cell clones are neither transiently nor randomly recruited into the inflammatory sites, but that they recognize some antigens which are associated with the pathogenesis of RA inflammation. Supporting this viewpoint, Mima *et al.* reported that T cell clones with an identical V_β CDR3 sequence frequently detected in the joints of some RA patients induced synovial hyperplasia in SCID mice when these clones were transferred (15).

In autoimmune disease murine models, it has been demonstrated that determinant spreading may be necessary for

Correspondence to: Y. Misaki; E-mail:misaki-tky@umin.ac.jp

Transmitting editor: S. Izui

Received 9 August 2003, *accepted* 3 October 2003

development of the full autoimmune syndrome (16–20). This epitope spreading occurs in experimental autoimmune encephalomyelitis, which is initiated by immunization of autoantigen peptides, as well as in NOD mice, a spontaneous autoimmune diabetes model. Both models are known to be mediated by T cells. This amplification of the autoimmune response by recruitment of T cells with additional specificities would lead to clonality diversification. Recently, it was reported that a shift towards a high-avidity pathogenic T cell population may be the key event in the progression of benign insulitis to overt diabetes in NOD mice (21). Alternatively, the clonality of the lesion might be restricted toward T cells which are able to accumulate preferentially and to surpass other clones, because of their advantage to expand clonally responding to the antigen released from the destroyed inflamed joint. Whether the clonality in the lesion continues to increase the diversity due to determinant spreading or decrease the variety is especially important in relation to T cell clonotype-targeted therapy. If the clonality becomes restricted, then regulation of a smaller number of clones should be sufficient to achieve antigen-specific immunotherapy. Thus, studies of the dynamics of clonality are of great significance.

So far, studies of T cell clonality have been performed using samples from patients with rather advanced disease. Although information on the dynamics of the clonality during the disease course from the early to the late stage could provide more profound insights into the pathogenic clones, kinetics studies of expanded clones in multiple joints at several time points throughout the disease course are not realistic, because of the difficulty of sampling during the long and heterogeneous clinical time course of RA. It is also difficult to appreciate and to compare the significance of expanded clones among patients, since RA patients are diverse and heterogeneous in terms of the disease severity, duration and modification by treatment.

Transgenic mice (Tg) carrying the env-pX region of the human T cell leukemia virus type I (HTLV-I) genome spontaneously develop chronic inflammatory arthritis as they age (22). The histopathologic characteristics of the joints of arthritic Tg closely resemble those found in patients with RA, showing proliferation of synovial lining cells, infiltration of inflammatory cells with lymph follicle-like structures, and formation of pannus-like granulation tissue with destruction of cartilage and subchondral bone (23). Genes for inflammatory cytokines, including IL-1α, IL-1β, IL-6, tumor necrosis factor-α, transforming growth factor-β1, IFN-γ and IL-2, as well as MHC genes are activated in joints. Moreover, these mice develop autoantibodies against IgG, type II collagen and heat-shock proteins (24). A T cell response to type II collagen (25) and loss of T cell tolerance in the periphery are also demonstrated (26). These pathological features are similar to those of RA. Therefore, the Tg are suitable for investigating T cell clonality during the disease course and its contribution to arthritis.

In the present study, using this spontaneous RA model HTLV-I env-pX Tg, we investigated the dynamics of the T cell clonotype in the affected four feet during the disease progression. We found clonally expanded T cells, some of which were common to all four inflamed feet. Surprisingly, as the disease progressed, the number of common clonotypes among the different feet increased, whereas the total number of clonotypes decreased. Adoptive transfer studies revealed that these common clonotypes of the donor feet migrated into the feet of the recipients, whose arthritis was exacerbated by the transfer. These results provide evidence that T cells in the inflamed joints are rather restricted to certain common clonotypes.

Methods

Mice

HTLV-I env-pX Tg were backcrossed to BALB/c mice for more than eight generations. The mice were maintained under specific pathogen-free conditions in the animal facility of the University of Tokyo, Graduate School of Medicine. All experiments using animals were performed according to the guidelines for animal experiments in our institution.

Clinical evaluation

The severity of arthritis was assessed using a clinical scoring system of 0–3: 0 = normal, 1 = redness and swelling, 2 = deformity, and 3 = ankylosis (27). Each foot was scored and the total score was determined; the maximum possible score per mouse was 12. Tg were divided into three groups by the arthritis stage: early stage (age: 5–10 weeks; score: 0–3), mid stage (age: 4–5 months; score: 6–8) and late stage (age: 7–8 months; score: 10–12).

Analysis of T cell clonality by RT-PCR/single-strand conformation polymorphism (SSCP)

Joint tissues were obtained from the front and back feet of Tg after removal of skin and muscle. Total RNA was prepared with Isogen (Nippon Gene, Tokyo, Japan) and then converted to cDNA with reverse transcriptase (Superscript II; Gibco/BRL, Gaithersburg, MD) and random hexamer oligonucleotide (Gibco/BRL) at 42°C for 2–3 h. PCR was performed with 100–200 ng of cDNA, 50 pmol of each of the 22 V_β primers and 50 pmol of a common C_β primer, dNTPs, and 1 U of Taq polymerase (Takara, Otsu, Japan) for 35 cycles (94°C for 1 min, 54°C for 2 min and 72°C for 3 min) in a Thermal Cycler 9600 (Perkin-Elmer, Norwalk, CT). The sequences of the V_β primers were obtained from published data (28). The sequence of C_β primer was 5′-GGCTCAAACAAGGAG-ACCTTG-3′. SSCP analysis was performed as follows. Amplified DNA was diluted (1:2–1:20) with a denaturing solution (95% formamide, 10 mM EDTA, 0.1% bromophenol blue and 0.1% xylene cyanol), heat denatured at 90°C for 2 min and electrophoresed on non-denaturing 4% polyacrylamide gels containing 10% glycerol. After electrophoresis, the DNA was transferred onto GeneScreen (NEB, Beverly, MA) and then hybridized with a biotinylated internal common C_β oligonucleotide probe (5′-AGGATCTGAGAAATGTGA-3′). The bound C_β probe was detected using a Phototope-Star detection kit (NEB).

The number of T cell clonotypes was calculated by three researchers independently who did not know the sample sources.

Standardization of TCR mRNA

To adjust the amount of TCR mRNA in spleen to that of joint for SSCP analysis, we conducted real-time quantitative PCR on the iCycler iQ real-time detection system (Bio-Rad, Hercules, CA). PCR was performed using QuantiTect SYBR Green PCR kit (Qiagen, Hilden, Germany) according to the manufacturer's instructions. For the amplification of the C_β region, 5′-GGTCTCCTTGTTTGAGCCAT-3′ was used as the 5′ primer and 5′-ACTGATGTTCTGTGTGACAG-3′ as the 3′ primer. The housekeeping gene β-actin (5′-TCACCCACACTGTGCCC-ATCTAC-3′, 5′-ACGATTTCCCTCTCAGCTGTGG-3′) was chosen for internal normalization.

Sequence analysis

TCR V_β genes extracted from SSCP polyacrylamide gels were re-amplified using the same TCR V_β and C_β primer as primary PCR. The re-amplified TCR V_β gene was subcloned to a plasmid vector (pGEM-T Easy Vector; Promega, Madison, MI). Nucleotide sequences of the TCR V_β genes were determined by the dideoxy method using a 310 Genetic Analyzer (Perkin-Elmer/Applied Biosystems, Foster, CA).

Adoptive transfer experiment

Spleens were removed aseptically from arthritic Tg in the late stage and control mice. As a control, we used non-arthritic Tg aged 4–6 weeks which had not developed the arthritis. Single-cell suspensions were prepared by teasing apart the spleens in HBSS and pushing them through a metal sieve with a syringe barrel. After washing with HBSS, $2–5\times10^7$ splenic cells were injected into either young Tg (6–7 weeks) with the onset of overt arthritis (the total score was <1–2) or BALB/c *nu/nu* mice. After 3 weeks, these recipients were sacrificed and then subjected to RT-PCR/SSCP analysis to examine the T cell clonotypes accumulated in the joints.

Statistical analysis

Data was analyzed using statistical software (Statcel, Saitama, Japan) and expressed as the mean ± SEM. The rate of common T cell clonotypes in all four feet and the arthritis score were compared by Student's *t*-test, and the total number of T cell clonotypes by Mann–Whitney's *U*-test.

Results

Accumulation of T cell clonotypes in arthritic joints of HTLV-I env-pX Tg

Arthritis in the Tg was discerned as swelling and redness of the footpad, including the ankle. The abnormality began to occur at age 4–8 weeks and thereafter the grade of arthritis increased as the animal aged. The clinical score finally reached the maximum at ~6 months (Fig. 1). Thus, since the disease severity was closely related to the age, we divided Tg into three groups according to their age, i.e. early stage (age: 5–10 weeks; score: 1–3), mid stage (age: 4–5 months; score: 6–8) and late stage (age: 7–8 months; score: 10–12).

We analyzed the T cell clonotypes infiltrating the joints of all four feet from HTLV-I env-pX Tg at 5 months (the mid stage) using the TCR/RT-PCR/SSCP method (Fig. 2). While the spleen exhibited smear patterns indicating a diverse T cell population consisting of heterogeneous CDR3 regions of TCR, accumulation of several distinct bands was observed in the feet. These results indicate that T cells expand oligoclonally in the joints of all four feet, as has been shown for the joints of RA patients.

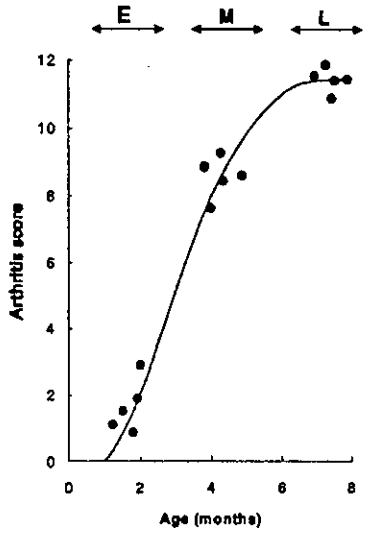

Fig. 1. Arthritic score increases with age of HTLV-I env-pX transgenic mice. The arthritic score starts to increase at age 4–8 weeks and reached the maximum score at ~6 months (n = 64). The arthritis was divided into three groups (early, mid and late stages) and five mice (solid circles) in each stage were used for T cell clonality analysis. E: early stage; M: mid stage; L: late stage.

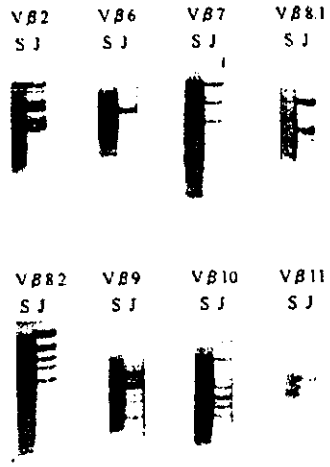

Fig. 2. Accumulation of T cell clonotypes in arthritic joints of HTLV-I env-pX transgenic mice analyzed by the RT-PCR/SSCP method. S: spleen. J: joint. TCR mRNA of spleen and joint were standardized by C_β products as described in Methods. The amount of TCR mRNA from all joints corresponded to ~1/16 of that from spleen. Thus, SSCP analysis was performed with PCR products using cDNA of spleen diluted by 1:16.

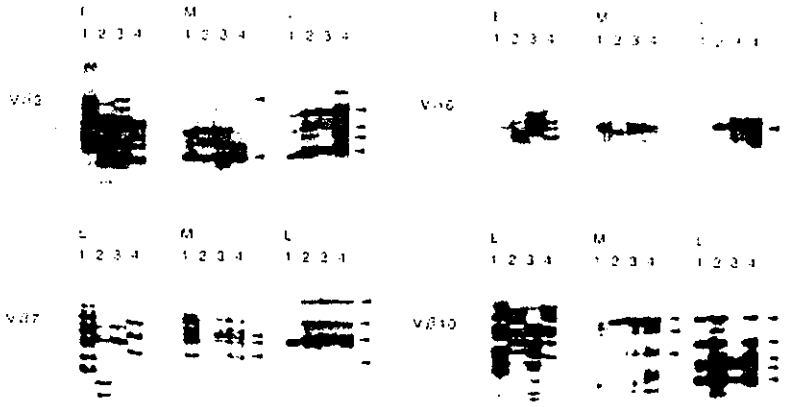

Fig. 3. Comparison of T cell clonotypes in the early, mid and late stages of arthritis. Lanes from 1 to 4 represent the right front foot, left front foot, right rear foot and left rear foot respectively. E: early stage; M: mid stage; L: late stage. Arrows indicate bands with identical migration in all four feet.

Table 1. Number of distinct T cell clonotypes accumulated in four feet of Tg in the early, mid and late stages[a]

Arthritis stage	V_β gene family																					Mean ± SEM	Percentage of common T cell clonotypes
	1	2	3	4	5.1	5.2	6	7	8.1	8.2	8.3	9	10	11	12	13	14	15	16	17	18		
E	–	0/8	–	0/7	–	–	1/6	1/10	0/7	1/7	2/6	0/7	3/12	0/5	–	1/7	1/7	2/8	1/4	1/7	2/6	1.0 ± 0.2/7.1 ± 0.5	14.1
M	–	3/7	–	1/8	–	–	1/4	1/10	3/6	2/5	3/4	2/8	4/11	1/5	–	2/7	1/10	0/7	2/6	0/9	1/4	1.7 ± 0.3/6.9 ± 0.6	24.6
L	–	4/5	–	1/6	–	–	3/3	4/5	3/4	4/5	4/4	5/9	8/10	2/4	–	2/6	1/7	3/7	2/4	3/10	1/5	3.1 ± 0.4/5.9 ± 0.5[b]	52.5

[a]T cell clonotypes were analyzed using three mice in each stage. Results are shown as common clonotypes/total clonotypes per foot (total number of bands in all four feet detected and the number of bands common to four feet were counted, and then divided by the number of feet to represent the value per foot). E: early stage; M: mid stage; L: late stage. –: bands were faint or not detected.
[b]$P < 0.05$.

The number of common T cell clonotypes increased, whereas the total number of T cell clonotypes decreased as the disease advanced

To investigate the change in T cell clonality during the progression of arthritis, we compared T cell clonotypes in the early, mid and late stages. The T cell clonotypes which accumulated in each joint of the four feet showed different mobility in the early stage, but they migrated to an identical position in the late stage (Fig. 3). Bands with the same mobility on SSCP gels had been demonstrated to possess the same nucleotide sequences (13,29,30) and we ourselves always confirm this rule by DNA sequencing. Therefore, bands with identical migration in SSCP represent identical clones.

We counted the total number of T cell clonotypes detected in each foot and the number of common clonotypes among the four feet. The results are summarized in Table 1. The proportion of T cell clonotypes common to all four feet was low in each V_β repertoire in the early stage (average 14.1%). However, it increased during progression of the stage. This increase during the transition from the early to late stage was observed in many V_β repertoires (V_β 2 and 6, $P < 0.0001$; V_β7, $P < 0.001$; V_β8.1 and 8.2, $P = 0.001$; V_β8.3, 10, 11 and 15, $P < 0.05$). Finally in the late stage, a high rate of >70% was found for V_β2, 6, 7, 8.1, 8.2, 8.3 and 10 (Fig. 4). Of interest, in contrast to the common clones, the total number of T cell clonotypes accumulated in joints decreased as the disease advanced ($P < 0.05$) (Table 1). In particular, V_β2, 6, 7 and 8.1 are striking, showing that the total number of T cell clonotypes in the late stage decreased by 40–50% compared with in the early stage. Taken together, the T cell clonotypes became identical while reducing their variety during progression of arthritis.

To examine amino acid sequences of the CDR3 region in common T cell clonotypes among four feet, DNA encoding the V_β genes were collected from SSCP gels and sequenced. As shown in Table 2, conserved amino acid motifs were found, e.g. QGW in the CDR3 region of V_β2 clones, RGTG in V_β9, and SXTGG, LTGG, QGA and YRG in V_β10. In addition, certain conserved amino acid motifs, such as RSG in V_β2 and V_β9, DWG in V_β2 and V_β10, and IQG and QGA in V_β10 and V_β11, were observed in the CDR3 region of different V_β clones. This sequence information implies the possibility that T cell clonotypes in multiple joints might recognize some common epitopes on antigens.

The common clones were able to migrate into the joints of the recipients

In order to investigate the pathological significance of the common clonotypes in four feet, we conducted an adoptive

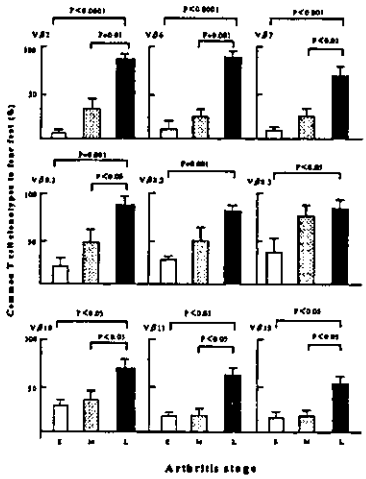

Fig. 4. The rate of common T cell clonotypes in all four feet increased as HTLV-I env-pX transgenic mice aged. The proportions of common T cell clonotypes in all four feet in the early, mid and late stages are demonstrated. Data given as the percentage of the number of bands common to all four feet against the total number of bands in all four feet. Values are expressed as the mean ± SEM (n = 5).

Table 2. The TCR VDJ region of common T cell clonotypes in four feet

V_β		N-D_β-N		J_β
V_β2	CSA	QGW	EQ	J_β2.6
V_β2	CSA	RSGRE	DTQ	J_β2.5
V_β2	CSA	RGI	SNERL	J_β1.4
V_β2	CS	IGQGW	GNTL	J_β1.3
V_β2	CS	EDWGG	AETL	J_β2.3
V_β9	CAS	RSGTI	SNERL	J_β1.4
V_β9	CAS	RGTGAN	TQ	J_β2.5
V_β9	CASS	RTGRG	EQ	J_β2.6
V_β9	CASS	RDR	SDY	J_β1.2
V_β9	CASS	RGTGQ	SYEQ	J_β2.6
V_β10	CASS	YQGAL	NQDTQ	J_β2.5
V_β10	CASS	VDWGD	QDTQ	J_β2.5
V_β10	CASS	SLTGG	YEQ	J_β2.6
V_β10	CASS	SGTGG	YEQ	J_β2.6
V_β10	CASS	IQGA	NSDY	J_β1.2
V_β10	CASS	YRGI	EQ	J_β2.6
V_β10	CASS	LTGGAD	TL	J_β2.4
V_β10	CASS	YRGP	NERL	J_β1.4
V_β11	CASS	LGQT	NSDY	J_β1.2
V_β11	CASS	SQGA	EV	J_β1.1
V_β11	CASS	IQG	TEV	J_β1.1

Underlined letters indicate conserved amino acid motifs.

transfer experiment. First, splenocytes derived from an arthritic Tg were transferred into nude mice. The joints of the feet of the recipients showed just mild swelling transiently. Nevertheless, clonotype analysis revealed that some common clones of the donors migrated into the feet of the recipients (Fig. 5).

Since non-T cell components are considered to be indispensable for inducing the persistent arthritis (31), we selected young Tg as recipients. In each experiment, splenic cells either from an arthritic Tg (experimental group) or a non-arthritic Tg (control group) were transferred into two young Tg with the onset of arthritis. Three weeks after the transfer, the arthritis score of the recipients from an arthritic Tg was significantly higher than that of recipients from non-arthritic Tg and that of non-treated Tg (Fig. 6). This result suggests that the progression of arthritis was accelerated by the transfer of splenocytes from arthritic mice and that the T cells from the donors were involved in the exacerbation of the arthritis. Three weeks after the transfer, these recipients were sacrificed and subjected to T cell clonality analysis. Some identical T cell clonotypes were detected in the donor and the two recipients, indicating that these identical T cell clonotypes accumulated in the joints of the recipients originated from the donors (Fig. 7). Since the smear pattern of the clonotype in the spleen of the recipients suggests that the degree of clonotype expansion is different between the joints and spleen, and since the common T cell clonotype between all four feet of the donor and recipient was not dominant in the spleen, we were able to rule out the possibility that the clonotype in joints simply reflects that of the spleen.

To verify that the clonotypes common to the donors and the recipients possess the identical TCR V_β chain sequences in transfer experiments, DNA was recovered from the bands with

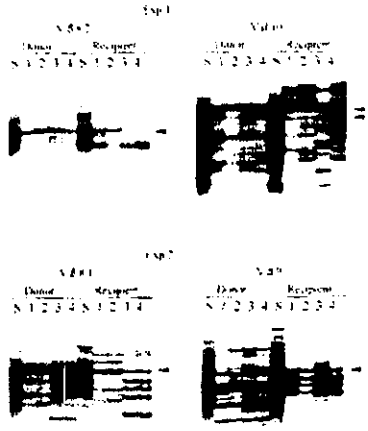

Fig. 5. The clonotype common to all four feet of a Tg donor migrated to the joints of nude mice. In each experiment, splenocytes from an arthritic Tg were transferred into a nude mouse recipient. Nude mice were sacrificed at 3 weeks after the cell transfer and subjected to T cell clonotype analysis. Representative V_β panels from two independent experiments are demonstrated. S: spleen. Lanes from 1 to 4 represent the right front foot, left front foot, right rear foot and left rear foot respectively. The common clones are indicated by the arrows. TCR mRNAs of spleen and joint were standardized by C_β products as described in Methods. The amount of TCR mRNA from all joints corresponded to ~1/10 of that from spleen.

same mobility on SSCP gels and sequences were determined. Table 3 shows the DNA sequences of SSCP bands from a donor and recipient, shown by arrows in Figs 5 and 7. As expected, the sequences were identical between the donor and recipient. These findings indicate that some of the common clonotypes in four feet of the donor infiltrated again

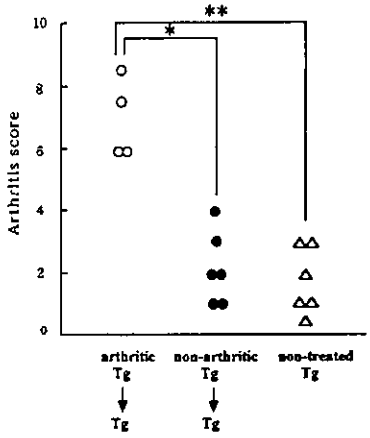

Fig. 6. Young Tg developed more severe arthritis after receiving splenocytes from an arthritic Tg. Splenocytes from an arthritic Tg or a non-arthritic Tg were transferred to young Tg on clinical onset, as described in Methods. The arthritis score at 3 weeks after cell transfer was judged. Note that the score of the recipients from an arthritic Tg (open circles) was significantly higher than that of recipients from a non-arthritic Tg (sold circles) and that of the non-treated Tg (open squares) ($^*P < 0.001$, $^{**}P < 0.0005$).

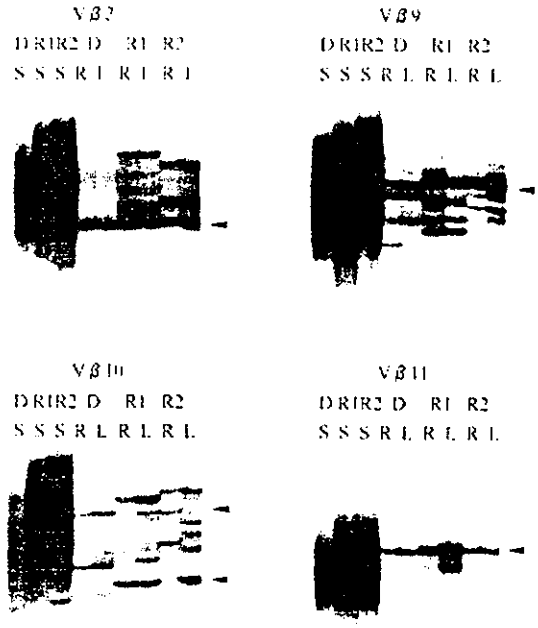

Fig. 7. The clonotype common to all four feet of an arthritic Tg donor migrated to the joints of young Tg recipients. Two young Tg were used as recipients in a transfer experiment. Recipients were sacrificed at 3 weeks after cell transfer and subjected to T cell clonality analysis. D: donor; R1: recipient 1; R2: recipient 2; S: spleen; R: right rear foot; L: left rear foot. Arrows indicate common T cell clonotypes among feet of the donor and two recipients. The amount of TCR mRNA from all joints corresponded to ~1/8 of that from spleen.

into the joints of the recipient. There were no clear conserved amino acids among migrated clonotypes in the amino acid sequences of the CDR3 region.

Discussion

We studied the T cell clonotypic change in arthritic joints of HTLV-I env-pX Tg during the development of the disease. In the early stage of the disease, T cell clonotypes diversified among the feet. On the contrary, in the late stage, most of the clonotypes were common to all four feet. The total number of accumulating clones decreased compared with in the early stage. Thus, the T cell clonotypes became identical and decreased in variety as the disease progressed. Some of these common clones remaining in the late stage joints might be arthrotropic, since the transfer studies revealed their ability to migrate into the joints. Due to the restricted availability of clinical samples, it might have been difficult to know the dynamic changes of clonality, which are diverse at the initial stage and finally are restricted to common clonotypes.

Analysis of T cell clonality in the joints of RA patients as well as in the affected organs of autoimmune disease animal models demonstrated the presence of common clonotypes among multiple joints or among different parts of an organ (13,28). Moreover, the amino acid sequences of TCR V_β junctional regions of clones which are identical in multiple joints of a patient were found to be the same as the sequences of the common clones of different patients (14). Considering that CDR3 interacts with the peptides presented by MHC molecules (32–34), these identical clones might recognize certain common antigens which are involved in the pathogenesis of RA. Our identification of common clonotypes in the four arthritic feet and some conserved CDR3 motifs among them is consistent with these previous findings.

In our present study of HTLV-I env-pX Tg, the accumulation of common clonotypes was distinct after the mid stage, whereas in the early stage it was not so pronounced. How can this change in clonality during disease progression be explained?

Several studies have implicated epitope spreading in the pathogenesis of autoimmune diseases (16–20). Disease progression is associated with a shifting of T cell autoreactivity from primary initiating self-antigenic determinants to defined cascades of secondary determinants that sustain the self-recognition involved in disease perpetuation. Intramolecular as well as intermolecular epitope spreading could presumably occur by antigen presentation of autoantigens derived from destroyed tissues (35–37). As recruitment of T cells specific for additional determinants continues, T cell clonality should become diversified. In our experiment, the early stage might fit the epitope-spreading model. The recruitment of T cells with other specificity proceeded independently in each joint. Since the time of onset of the arthritis is different among the four feet, it is also possible that the degree of autoimmune response propagation differs in each foot, resulting in the accumulation of different clones in each joint. The autoantigens driving the autoimmune response in each joint may differ in this stage. However, epitope spreading may not explain the T cell behavior in our arthritis model throughout the entire course of the disease, since the total number of T cell clones

Table 3. The TCR VDJ region of T cell clonotypes common to donor and recipient in the transfer experiments[a]

	V_β	N-D_β-N	J_β	
(A)				
Exp. 1				
V_β8.2	TGTGCCAGC	GGTGATTCCGGGACAG	CAAACTCCGACTAC	J_β1.2
	C A S	G D S G T A	N S D Y	
V_β10	TGTGCCAGCAGC	TTACTGGGGGGGCGC	AGTGCAGAAACGCTG	J_β2.3
	C A S S	L L G G R	S A E T L	
	TGTGCCAGCAGC	TTGGGGACT	AGTGCAGAAACGCTG	J_β2.3
	C A S S	L G T	S A E T L	
Exp. 2				
V_β8.1	TGTGCCAGCAG	CCGACAGTTT	TCCAACGAAAGATTA	J_β1.4
	C A S S	R Q F	S N E R L	
V_β9	TGTGCTAGCAGT	AGACAGGGG	TATGAACAG	J_β2.6
	C A S S	R Q G	Y E Q	
(B)				
V_β2	TGCAGTG	CTCAGGGGTGG	GAACAG	J_β2.6
	C S A	Q G W	E Q	
V_β9	TGTGCTAGCAGT	AGAACAGGGAGAGGT	GAACAG	J_β2.6
	C A S S	R T G R G	E Q	
	TGTGCTAGCAG	GGGCACAGGGGCAA	ACACCCAG	J_β2.5
	C A S	R G T G A N	T Q	
V_β10	TGTGCCAGCAGC	TACCAGGGGGCACTT	AACCAAGACACCCAG	J_β2.5
	C A S S	Y Q G A L	N Q D T Q	
V_β11	TGTGCAAGCAGC	ATACAGGGA	ACAGAAGTC	J_β1.1
	C A S S	I Q G	T E V	

[a]The similar electrophoretic mobility bands in donor and recipient indicated by arrows in Figs 5 and 7 were cut out and subcloned after PCR amplification. Their sequences were determined. (A) Transfer experiment in nude mice. (B) Transfer experiment in young Tg.

decreased and the identity of clonality increased with disease progression.

It is shown that the TCR repertoire of memory cells which expand selectively during the recall response are rather restricted (38). Thus, such clones might be increasing while an autoantigen repetitively stimulates and drives the (pathogenic) immune response. Adding to this, some autoreactive T cell clones might be inactivated or deleted by regulatory mechanisms. Therefore, we may reason that the number of accumulating clones in the lesion of an autoimmune disease might gradually decrease, leaving clones which are able to expand more efficiently or are less susceptible to cell death.

Alternatively, the clonal restriction in the joints might reflect avidity maturation of a T cell population. Amrani *et al.* demonstrated that a shift towards a high-avidity pathogenic T cell population may be the key event in the progression of benign insulitis to overt diabetes using NOD mice (21). Applying this hypothesis, we tend to prefer that some of the remaining common clonotypes have an advantage in clonal expansion due to their higher avidity for certain autoantigens and are related to the inflammation of the joints. However, it is too early to conclude that the remaining common clonotypes are pathogenic, since other clones might also be involved in the exacerbation of young Tg arthritis after the transfer.

Nevertheless, some of them are at least arthrotropic since they migrated to the joints of the recipients, implying that they recognize a certain autoantigen in the joint. Since it has indeed been demonstrated that dominant T cell clones in Tg recognize collagen type II (25), Tax and Env of the pX products (39), it would be of great interest to investigate whether these common clones respond to those antigens.

Taken together, during the perpetuation of arthritis, T cell clonality decreased in variety and was restricted to the clones, some of which are arthrotropic and might be related to the pathogenesis of arthritis. This 'clonal restriction' phenomena should be verified in other autoimmune diseases and its models to develop antigen-specific immunotherapy targeting certain common T cell clonotypes.

Acknowledgements

This work was supported by a Grant-in-Aid for Scientific Research from the Ministry of Education, Culture, Sports, Science and Technology, and Grants from the Ministry of Health, Labor and Welfare.

Abbreviations

HTLV-I	human T cell leukemia virus type I
RA	rheumatoid arthritis
SSCP	single-strand conformation polymorphism
Tg	transgenic mouse

References

1 Nepom, G. T., Byers, P., Seyfried, C., Healey, L. A., Wilske, K. R., Stage, D. and Nepom, B. S. 1989. HLA genes associated with rheumatoid arthritis: identification of susceptibility alleles using specific oligonucleotide probes. *Arthritis Rheum.* 32:15.

2 Weyand, C. M., McCarthy, T. G. and Goronzy, J. J. 1995. Correlation between disease phenotype and genetic heterogeneity in rheumatoid arthritis. *J. Clin. Invest.* 95:2120.

3 Weyand, C. M. and Goronzy, J. J. 1999. HLA polymorphisms and T cells in rheumatoid arthritis. *Int. Rev. Immunol.* 18:37.

4 Van Boxel, J. A. and Paget, S. A. 1975. Predominantly T-cell

infiltrate in rheumatoid synovial membranes. *N. Engl. J. Med.* 293:517.
5 Goronzy, J. J. and Weyand, C. M. 1995. T cells in rheumatoid arthritis. Paradigms and facts. *Rheum. Dis. Clin. North Am.* 21:655.
6 Panayi, G. S., Lanchoury, J. S. and Kingsley, G. H. 1992. The importance of the T cell in initiating and maintaining the chronic synovitis of rheumatoid arthritis. *Arthritis Rheum.* 35:729.
7 Gary, S. F. and Nathan, J. Z. 2002. How important are T cells in chronic rheumatoid synovitis? II. T cell-independent mechanisms from beginning to end. *Arthritis Rheum.* 46:298.
8 Stamenkovic, I., Stegagno, M., Wright, K. A., Krane, S. M., Amento, E. P., Colvin, R. B., Duquesoy, R. J. and Kurnick, J. T. 1988. Clonal dominance among T-lymphocyte infiltrates in arthritis. *Proc. Natl Acad. Sci. USA* 85:1179
9 Paliard, X., West, S. G., Lafferty, J. A., Clements, J. R., Kappler, J. W., Marrack, P. and Kotzin, B. L. 1991. Evidence for the effects of a superantigen in rheumatoid arthritis. *Science* 253:325.
10 Struyk, L., Hawes, G. E., Chatila, M. K., Breedveld, F. C., Kurnick, J. T. and van den Elsen, P. J. 1995. T cell receptors in rheumatoid arthritis. *Arthritis Rheum.* 38:577.
11 Gonzalez-Quintial, R., Baccala, R., Pope, R. M. and Theofilopoulos, A. N. 1996. Identification of clonally expanded T cells in rheumatoid arthritis using a sequence enrichment nuclease assay. *J. Clin. Invest.* 97:1335.
12 Yamamoto, K., Sakoda, H., Nakajima, T., Kato, T., Okubo, M., Dohi, M., Mizushima, Y., Ito, K. and Nishioka, K. 1992. Accumulation of multiple T cell clonotypes in the synovial lesions of patients with rheumatoid arthritis revealed by a novel clonality analysis. *Int. Immunol.* 4:1219.
13 Ikeda, Y., Masuko, K., Nakai, Y., Kato, T., Hasunuma, T., Yoshino, S., Mizushima, Y., Nishioka, K. and Yamamoto, K. 1996. High frequencies of identical T cell clonotypes in synovial tissues of rheumatoid arthritis patients suggest the occurrence of common antigen-driven immune responses. *Arthritis Rheum.* 39:446.
14 Kurokawa, M., Kato, T., Masuko-Hongo, K., Ueda, S., Kobata, T., Okubo, M., Nishimaki, T., Akaza, T., Yoshino, S., Kasukawa, R., Nishioka, K. and Yamamoto, K. 1999. Characterization of T cell clonotypes that accumulated in multiple joints of patients with rheumatoid arthritis. *Ann. Rheum. Dis.* 58:546.
15 Mima, T., Ohshima, S., Sasai, M., Nishioka, K., Shimizu, M., Murata, N., Yasunami, R., Matsuno, H., Suemura, M., Kishimoto, T. and Saeki, Y. 1999. Dominant and shared T cell receptor â chain variable regions of T cells inducing synovial hyperplasia in rheumatoid arthritis. *Biochem. Biophys. Res. Commun.* 263:172.
16 Lehmann, P. V., Forsthuber, T., Miller, A. and Sercarz, E. E. 1992. Spreading of T cell autoimmunity to cryptic determinants of an autoantigen. *Nature* 358:155.
17 Lehmann, P. V., Sercarz, E. E., Forsthuber, T., Dayan, C. M. and Gammon, G. 1993. Determinant spreading and the dynamics of the autoimmune T cell repertoire. *Immunol. Today* 14:203.
18 McRae, B. L., Vanderlugt, C. L., DalCanto, M. C. and Miller, S. D. 1995. Functional evidence for epitope spreading in the relapsing pathology of experimental autoimmune encephalomyelitis. *J. Exp. Med.* 182:75.
19 Tuohy, V. K., Yu, M., Yin, L., Kawczak, J. A., Johnson, J. M., Mathisen, P. M., Weinstock-Guttman, B. and Kinkel, R. P. 1998. The epitope spreading cascade during progression of experimental autoimmune encephalomyelitis and multiple sclerosis. *Immunol. Rev.* 164:93.
20 Kaufman, D. L., Clare-Salzler, M., Tian, J., Forsthuber, T., Ting, G. S., Robinson, P., Atkinson, M. A., Sercarz, E. E., Tobin, A. J. and Lehmann, P. V. 1993. Spontaneous loss of T cell tolerance to glutamic acid decarboxylase in murine insulin-dependent diabetes. *Nature* 366:69.
21 Amrani, A., Verdaguer, J., Serra, P., Tafuro, S., Tan, R. and Santamaria, P. 2000. Progression of autoimmune diabetes driven by avidity maturation of a T cell population. *Nature* 406:739.
22 Iwakura, Y., Tosu, M., Yoshida, E., Takiguchi, M., Sato, K., Kitajima, I., Nishioka, K., Yamamoto, K., Takeda, T., Hatanaka, M., Yamamoto, H. and Sekiguchi, T. 1991. Induction of inflammatory arthropathy resembling rheumatoid arthritis in mice transgenic for HTLV-I. *Science* 253:1026.
23 Yamamoto, H., Sekiguchi, T., Itagaki, K., Saijo, S. and Iwakura, Y. 1993. Inflammatory polyarthritis in mice transgenic for human T cell leukemia virus type I. *Arthritis Rheum.* 36:1612.
24 Iwakura, Y., Saijo, S., Kioka, Y., Nakayama-Yamada, J., Itagaki, K., Tosu, M., Asano, M., Kanai, Y. and Kakimoto, K. 1995. Autoimmunity induction by human T cell leukemia virus type 1 in transgenic mice that develop chronic inflammatory arthropathy resembling rheumatoid arthritis in humans. *J. Immunol.* 155:1588.
25 Kotani, M., Tagawa, Y. and Iwakura, Y. 1999. Involvement of autoimmunity against type II collagen in the development of arthritis in mice transgenic for the human T cell leukemia virus type I *tax* gene. *Eur. J. Immunol.* 29:54.
26 Kishi, S., Saijo, S., Arai, M., Karasawa, S., Ueda, S., Kannagi, M., Iwakura, Y., Fujii, M. and Yonehara, S. 1997. Resistance to fas-mediated apoptosis of peripheral T cells in human T lymphocyte virus type I (HTLV-I) transgenic mice with autoimmune arthropathy. *J. Exp. Med.* 186:57.
27 Osman, G. E., Toda, M., Kanagawa, O. and Hood, L. E. 1993. Characterization of the T cell receptor repertoire causing collagen arthritis in mice. *J. Exp. Med.* 177:387.
28 Komagata, Y., Masuko, K., Tashiro, F., Kato, T., Ikuta, K., Nishioka, K., Ito, K., Miyazaki, J. and Yamamoto, K. 1996. Clonal prevalence of T cells infiltrating into the pancreas of prediabetic non-obese diabetic mice. *Int. Immunol.* 8:807.
29 Okubo, M., Kurokawa, M., Ohto, H., Nishimaki, T., Nishioka, K., Kasukawa, R. and Yamamoto, K. 1994. Clonotype analysis of peripheral blood T cells and autoantigen-reactive T cells from patients with mixed connective tissue disease. *J. Immunol.* 153:3784.
30 Yamamoto, K., Masuko, K., Takahashi, S., Ikeda, Y., Kato, T., Mizushima, Y., Hayashi, K. and Nishioka, K. 1995. Accumulation of distinct T cell clonotypes in human solid tumors. *J. Immunol.* 154:1804.
31 Saijo, S., Kotani, M., Habu, K., Ishitsuka, C., Yamamoto, H., Sekiguchi, T. and Iwakura, Y. 1999. Bone marrow-derived cells are responsible for the development of autoimmune arthritis in human T cell leukemia virus type I-ransgenic mousetransgenic mice and those of normal mice can suppress the disease. *J. Immunol.* 163:5700.
32 Garboczi, D. N., Ghosh, P., Utz, U., Fan, Q. R., Biddison, W. E. and Wiley, D. C. 1996. Structure of the complex between human T cell receptor, viral peptide and HLA-A2. *Nature* 384:134.
33 Dessen, A., Lawrence, C. M., Cupo, S., Zaller, D. M. and Wiley, D. C. 1997. X-ray crystal structure of HLA-DR4 (DRA*0101, DRB1*0401) complexed with a peptide from human collagen II. *Immunity* 7:473.
34 Garcia, K. C., Degano, M., Stanfield, R. L., Brunmark, A., Jackson, M. R., Peterson, P. A., Teyton, L. and Wilson, I. A. 1996. An αβT cell receptor structure at 2.5 A and its orientation in the TCR-MHC complex. *Science* 274:209.
35 Craft, J. and Fatenejad, S. 1997. Self antigens and epitope spreading in systemic autoimmunity. *Arthritis Rheum.* 40:1374.
36 McCluskey, J., Farris, A. D., Keech, C. L., Purcell, A. W., Rischmueller, M., Kinoshita, G., Reynolds, P. and Gordon, T. P. 1998. Determinant spreading: lessons from animal models and human disease. *Immunol. Rev.* 164:209.
37 Mamula, M. J. 1998. Epitope spreading: the role of self peptides and autoantigen processing by B lymphocytes. *Immunol. Rev.* 164:231.
38 McHeyzer-Williams, L. J., Panus, J. F., Mikszta, J. A. and McHeyzer-Williams, M. G. 1999. Evolution of antigen-specific T cell receptors *in vivo*: preimmune and antigen-driven selection of preferred complementarity-determining region 3 (CDR3) motifs. *J. Exp. Med.* 189:1823.
39 Fujisawa, K., Okamoto, K., Asahara, H., Hasunuma, T., Kobata, T., Kato, T., Sumida, T. and Nishioka, K. 1998. Evidence for autoantigens of Env/Tax proteins in human T cell leukemia virus type I Env-pX transgenic mice. *Arthritis Rheum.* 41:101.

International Immunology, Vol. 16, No. 3, pp. 423–431
doi: 10.1093/intimm/dxh046

Development of TCRB CDR3 length repertoire of human T lymphocytes

Junko Nishio[1], Mihoko Suzuki[1], Toshihiro Nanki[1], Nobuyuki Miyasaka[1] and Hitoshi Kohsaka[1]

[1]Department of Bioregulatory Medicine and Rheumatology, Graduate School, Tokyo Medical and Dental University, 1-5-45 Yushima, Bunkyo-ku, Tokyo 113-8519, Japan

Keywords: gene rearrangement, peripheral blood, thymus

Abstract

The third complementarity-determining region (CDR3) of TCR interacts directly with antigenic peptides bound to grooves of MHC molecules. Thus, it is the most critical TCR structure in launching acquired immunity and in determining fates of developing thymocytes. Since length is one of the components defining the CDR3 heterogeneity, the CDR3 length repertoires have been studied in various T cell subsets from humans in physiological and pathological conditions. However, how the CDR3 length repertoire develops has been addressed only by a few reports, including one showing that CDR3 of CD4 thymocytes becomes shorter during thymic development. Here, we explored multiple regulations on the development of the TCRB CDR3 length repertoires in the thymus and the peripheral blood. CDR3 length spectratyping was employed to examine thymocyte and peripheral T cell populations for their CDR3 length repertoires. We have found that repertoire distribution patterns depend on use of the BV gene. The BV-dependent patterns were shaped during thymic selections and maintained in the peripheral blood. Differences in the mean CDR3 length among different BV subsets were seen throughout lymphocyte development. We also observed that CDR3 was shortened in both CD4 and CD8 thymocytes. Of note, the degrees of the shortening depended on the CD4/CD8 lineage and on use of the BV gene. When expansions of peripheral T cell clones are negligible, no obvious difference was seen between mature thymocytes and peripheral lymphocytes. Thus, the TCRB CDR3 length repertoires are finely tuned in the thymus before the lymphocytes emigrate into the peripheral blood.

Introduction

Using surface receptors for antigens, αβ T cells recognize antigenic peptides bound to MHC class I or II molecules. Studies using X-ray crystallography have demonstrated that three-dimensional structures composed by the first, second and third complementarity-determining regions (CDR1, 2 and 3) of TCR α and β chains interact directly with peptides presented by the MHC molecules (1,2). Avidity of the interaction is defined by topological structure and location of charged amino acid residues of the interface peptides (3). In the TCR chain, CDR3 nucleic acid sequence is most diverse because it is generated by recombination of multiple V, D (in the case of TCRβ) and J gene segments, and by random addition of interlocating N region nucleotides (4,5). Since this region interacts most closely with the antigenic peptide, the diversity of the CDR3 amino acid sequences accounts for a wide array of antigen specificities within the functional T cell repertoire.

The molecular interaction of interface peptides is similarly important in association between antigenic peptides and MHC molecules. This interaction limits heterogeneity of peptides that can bind to the products of a given MHC allele (6). The length of the antigenic peptides is also restricted by interaction with MHC and with TCR (6). In contrast, the TCR CDR3 segments are more diverse in length. This might be explained by weaker association of antigenic peptides with TCR than with MHC (3,7). However, it remains to be seen how the CDR3 length repertoire is regulated during thymic development and in peripheral blood.

The αβ T cell repertoire develops through a number of selection steps in the thymus. TCRB gene rearrangement becomes complete first at the stage of $CD3^-CD4^+CD8^-$ immature single-positive (CD4 ISP) thymocytes (8,9). If their TCRB genes rearrange in-frame and their products pair successfully with pre-Tα chains, these cells survive and

Correspondence to: H. Kohsaka; E-mail: kohsaka.rheu@tmd.ac.jp

Transmitting editor: K. Yamamoto

Received 25 August 2003, *accepted* 25 November 2003

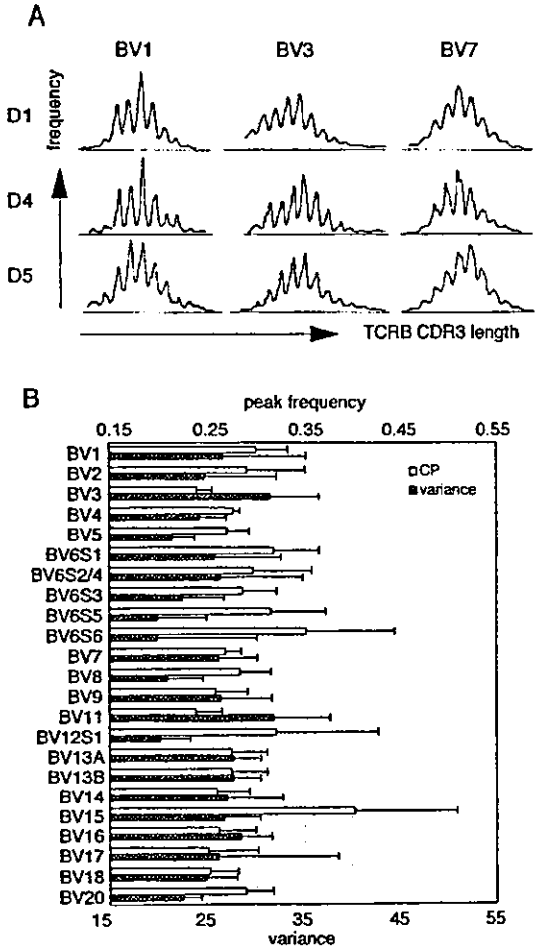

Fig. 1. BV-dependent differences in TCRB CLS histogram. (A) The histograms of the BV1, 3 and 7 subsets of peripheral CD4 T cells from three donors (D1, D4 and D5). (B) The CP frequencies and the variances in the individual BV subsets. They were calculated using TCRB CLS histograms of peripheral CD4 T cells from six child donors. The classification of the BV families was based on the definition by the WHO/International Union of Immunological Societies, Nomenclature Subcommittee on TCR Designation (30). The open columns and shaded columns represent the mean values of the CP frequencies and those of the variances respectively. The bars show their SD.

proliferate to become $CD4^+CD8^+$ double-positive thymocytes (8,10). They express TCRβ chains together with products of the in-frame rearranged TCRA gene. The double-positive thymocytes then undergo positive and negative selection, which make mature CD4 and CD8 T cell repertoires desirable to eliminate foreign pathogens. Although these processes are directed by the avidity of TCR with its ligand (11), their effects on the CDR3 length repertoire have hardly been explored.

The heterogeneity of the TCR CDR3 length in T cells at any developmental stages can be tested with TCR CDR3 length spectratyping (CLS). This method visualizes the distribution of TCR CDR3 length as histograms (12). It has been shown that typical histograms that are derived from mature peripheral T lymphocyte pools display a Gaussian-like distribution with 3-base spacing. If a histogram is biased by an unexpectedly high frequency at a specific length, it indicates that the studied population contains an expanded T cell clone whose CDR3 has the corresponding length. Based on this, the TCR CLS technique has been employed to study clonal perturbation of T cell repertoires from healthy donors and patients with various inflammatory diseases (13–19). The results have given us some insights into the physiology and pathology of T cell homeostasis.

The above facts all indicate the importance of discerning how heterogeneity of the CDR3 length repertoire is physiologically regulated, especially in the thymus. No gross difference in CDR3 length distribution between fetal and adult T cell pools has been reported (20). Yassai *et al.* (21) reported that thymocytes with shorter TCRB CDR3 are selected during transition from $CD4^+CD8^+$ thymocytes to CD4 SP thymocytes. Their subsequent report used murine systems to show that the shortening is mediated by TCR–peptide–MHC interaction in the thymus (22). Of note, they suggested that human repertoires might be under distinct regulation. Other investigators have described that different TCRB CDR3 lengths were preferred by different BV and BJ combinations in mice (23), and BJ genes in humans (24). However, no studies have addressed which stages in lymphocyte development are responsible for these differences.

How are the CDR3 length repertoires of various T cell subsets formed, modulated and maintained in the thymus and in the peripheral blood? How does the shortening occur in the human thymus? The present study was conducted to address these issues. By examining thymocytes and peripheral T cells for TCR CLS patterns, we have found that formation of human TCR CDR3 length repertoires is under multiplex regulations in the thymus.

Methods

Samples

Thymic fragments and peripheral blood were collected from child donors during heart surgery for correction of congenital cardiac anomalies. They were from 1 to 13 years old (mean 5.6 years old). They suffered from no immunological or hematological disorders. Consent forms were obtained before the operation. CD4 ISP thymocytes, mature CD4 and CD8 SP thymocytes, and peripheral CD4 and CD8 T lymphocytes were sorted from the thymic tissues or peripheral lymphocytes as described previously (25). Purities of the separated cells were >94%.

PCR

RNA were extracted from the sorted thymocytes and lymphocytes, and converted to cDNA (25). To amplify TCR transcripts with individual TCRBV family genes, the cDNA were subjected to PCR using a fluorescent TCRBC-specific anti-sense primer ($C_\beta b$) and a panel of sense oligonucleotide primers specific to TCRBV gene families (26). The amplification reaction consisted of 35 cycles of 1 min at 94°C, 1 min at 60°C and 1 min at 72°C, with final extension at 72°C for 7 min.

To amplify TCR transcripts with individual members of the BV7 family (BV7S1, BV7S2 and BV7S3 genes), a sense primer specific to the three BV7 family genes ($V_\beta 7os$: GGA GCT CAT

GTT TGT CTA CA) and a BC-specific antisense primer [C_βa (26)] were used for primary PCR. The reaction consisted of 25 cycles of 1 min at 94°C, 1 min at 53°C and 1 min at 72°C followed by final extension at 72°C for 7 min. Part of the products were further amplified with a nested sense primer specific to BV7S1, BV7S2 or BV7S3 genes (V_β7S1s: TAC AGC TAT GAG AAA CTC TC; V_β7S2s: TAC AGT CTT GAA GAA CGG GT; or V_β7S3s: TCT ACA ACT TTA AAG AAC AGA C) and the fluorescent C_βb primer. The reaction consisted of 25 cycles of 1 min at 94°C, 1 min at 53°C and 1 min at 72°C followed by final extension at 72°C for 7 min.

TCR CLS

The PCR products were fractionated on denaturing 7% polyacrylamide gel in a Hitachi SQ-5500 sequencer (Hitachi Electronics Engineering, Tokyo, Japan). The data were analyzed with the associated software to display histograms. Relative percentage of the TCRB transcripts of a given length to total TCRB transcripts in the BV subsets, which is called the frequency in this report, was calculated by dividing the fluorescence intensity of the corresponding peaks by the sum of the intensity of all peaks.

Statistical analyses

CDR3 length, defined as previously described (20), ranged from 6 to 60 bases. Nineteen frequency values within this range were treated as variables for cluster analyses, which were performed with Statistica 4.1J (Tulsa, OK). The variances were calculated as follows: $\sum_{n=2}^{20} F_{3n} \times (L_{3n} - \text{mean CDR3 length})^2$, where F_{3n} stands for the frequency value that corresponds to a given CDR3 length of L_{3n}. The Kruskal–Wallis test was used to compare the central peak (CP) frequencies, variances and mean CDR3 lengths of the histograms of different BV subsets. The Mann–Whitney test was used to compare these parameters of the histograms of the CD4 ISP thymocytes with those of the other populations.

Results

BV-dependent TCRB CDR3 length repertoires of peripheral CD4 T cells

In order to characterize unbiased TCRB CDR3 length repertoires of the mature T lymphocytes, peripheral CD4 T lymphocytes from six child donors were examined. This population was studied because biases of the T cell repertoires by clonally expanded T cells are more frequent in elder individuals and in the CD8 T cell pool (13,15,27,28). Although the histogram of each BV subset displayed a Gaussian-like distribution without outstanding biases, different BV subsets had slightly different patterns. Histograms of BV1, 3 and 7 gene families of three donors are shown to represent such differences (Fig. 1A). The shapes of different BV subsets were distinguished by the height of the CP that always had the highest frequency and by the width of the span. The histograms of BV1 had a high CP and narrow span, those of BV3 had a low CP and wide span, and BV7 had modestly high CP and a narrow span.

The characteristics were quantitatively assessed with the CP frequencies and the variances; the variances indicate span of the histograms. These two values were calculated for all BV subsets studied (Fig. 1B). Various combinations of CP frequencies and variances were observed. Reflecting the histogram pattern of the BV3 subset, its CP frequencies were low and the variances were remarkably large. This was also the case with the BV11 subset. The BV1 subset, as well as the BV6S1 subset, had high CP frequencies and small variances. The two parameters also describe the characteristics of the BV7 subset: moderate CP frequency and small variance.

Although some BV subsets had higher CP frequencies than BV1, or smaller variances than BV1 and 7, the BV1, 3 and 7 subsets were further studied to investigate how these differences develop during T lymphocyte development. The other BV subsets occasionally had minor and random biases, which should be due to small expansions of T cell clones. The characteristics of the three BV subsets and similarity within the same subsets could be illuminated by line graphs of the CDR3 length repertoires from six donors (Fig. 2A). Statistical comparison of the CP frequencies and the variances among the three subsets from six donors demonstrated that the CP frequencies of the BV1 subset were highest, while those of the BV3 subset were lowest, and that the variances in the BV3 subset were largest (Fig. 3A and B).

Pannetier *et al.* (23) reported that the mean TCRB CDR3 length of murine lymphocytes depends on use of BV genes. This was the case with human peripheral lymphocytes; the mean length of the TCRBV7 transcripts was longest, while that of the TCRBV3 transcripts was shortest (Fig. 3C).

Overall differences in the CLS patterns were elucidated by cluster analysis, which treated 19 frequency values at 6–60 bases as variables. A total of 18 histograms from six donors were segregated into three groups, each of which contained histograms of BV1, 3 or 7 subsets (Fig. 4A).

According to the published database, the BV7 family consists of BV7S1, 7S2 and 7S3 genes, while BV1 and 3 families have a single gene member (29). The histograms of the BV7 subset were derived from the PCR products that were generated with a primer specific to all BV7 family genes. In order to examine the TCR transcripts with individual BV7 genes, these transcripts were independently amplified with specific primers. The CLS distributions of the transcripts with the three BV7 genes were homologous and no statistical differences in CP frequency, variance or mean TCR length were observed (data not shown). Thus, the BV7 family subset was analyzed as a whole in the present studies.

Development of the BV-dependent repertoires in the thymus

TCRBV1, 3 and 7 transcripts that were derived from CD4 ISP thymocytes, and CD4 and CD8 SP thymocytes from the same set of donors were analyzed to study how the BV-dependent characteristics develop. As was discussed in our previous report (25), the CD4 ISP thymocytes have undergone TCRB gene rearrangement, but have not started positive or negative selection. Thus, unlike CD4 CD8 double-positive cells, a part of which are already under pressure of thymic selection, they are the best for investigation of primordial TCR repertoires.

The histograms of the CD4 and CD8 SP thymocytes shared the same characteristics as those of the peripheral CD4 cells

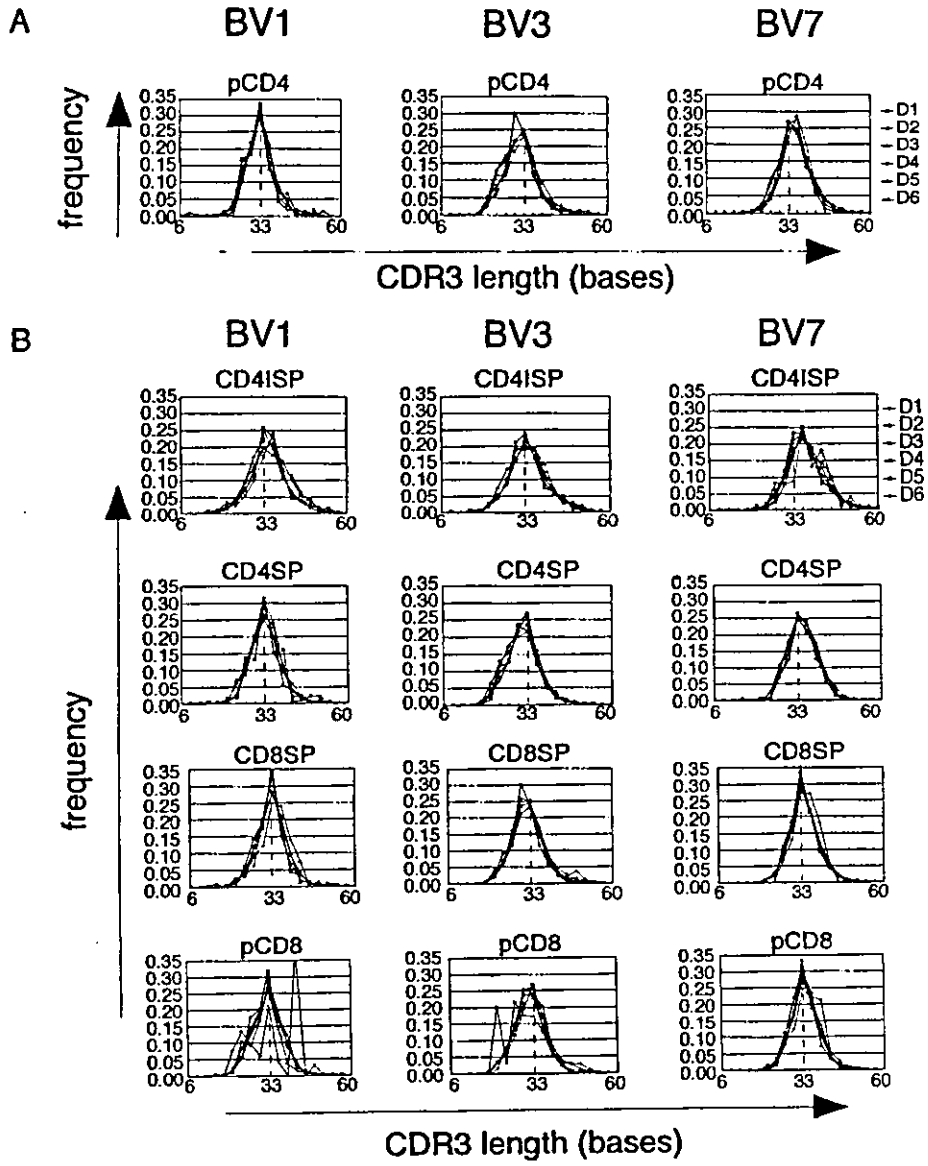

Fig. 2. TCRB CLS histograms of the BV1, 3 and 7 subsets of the peripheral lymphocytes and thymocytes. Distributions of the frequencies are presented in a line graph format. The data of the six donors (D1–D6) are shown as overlaid line graphs in each panel to illuminate BV-specific characteristics. (A) The histograms of the three BV subsets in their peripheral CD4 T cells. (B) The histograms of the CD4 ISP, CD4 SP and CD8 SP thymocytes, and peripheral CD8 T cells. Except for the CD4 ISP thymocytes, the histograms of each BV subset were similar. The BV1 and 3 subsets of the peripheral CD8 T cells from D4 were considerably biased, probably because of clonal expansions.

(Fig. 2B). In both SP populations, the CP frequencies of the BV1 subset were highest and those of the BV3 subset were lowest. The variances in the BV3 subset were largest. These differences were statistically significant (Fig. 3A and B).

Peripheral CD8 T cells from the same donors were analyzed in the same way. Their histograms were often biased since CD8 T cells are prone to large clonal expansions. Nevertheless, the BV-dependent characteristics were held well by the peripheral CD8 T cells (Figs 2B, and 3A and B).

In contrast, differences among the three subsets were not significant in the histograms of the CD4 ISP thymocytes (Fig. 2B). These histograms shared the same features, which were characterized by low CP and wide span regardless of BV gene use. In all of the three BV subsets, the CP frequencies and variances of the CD4 ISP thymocytes were different from those of the SP thymocytes and peripheral T cells in a statistically significant manner (Fig. 3A and B). The CP frequencies of CD4 ISP were significantly lower than those of CD4 SP in the BV1, 3, and 7 subsets ($P < 0.01$, $P < 0.05$ and $P < 0.05$ respectively), than those of CD8 SP ($P < 0.01$ for each subset), than those of peripheral CD4 ($P < 0.01$, $P < 0.05$ and $P < 0.01$ respectively) and than those of peripheral CD8 ($P < 0.01$, $P < 0.05$ and $P < 0.01$ respectively). The variances of CD4 ISP were significantly larger than those of CD4 SP in the

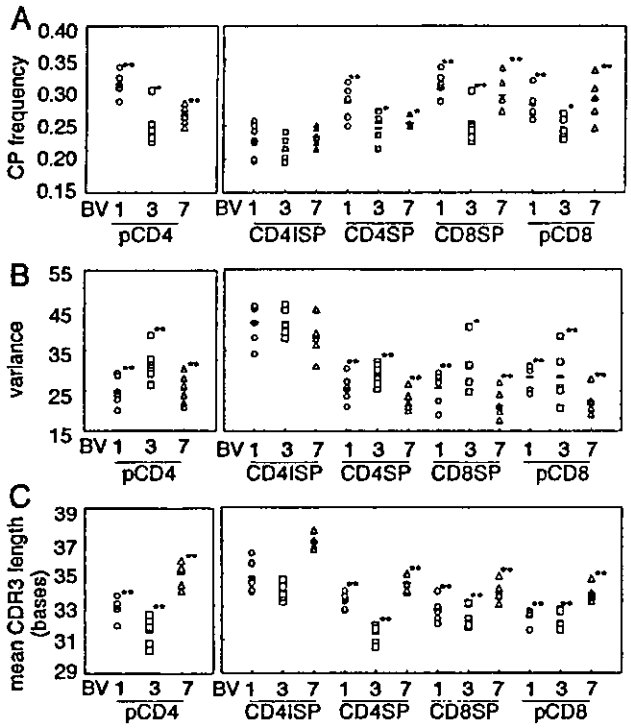

Fig. 3. Parameters to compare the TCR CLS histograms of CD4 ISP, CD4 SP and CD8 SP thymocytes, and peripheral CD4 and CD8 T cells. CP frequencies (A), variances (B) and mean CDR3 lengths (C) in the BV1, 3 and 7 subsets from the six donors are shown. Those of the peripheral CD8 T cells from D4 are excluded because of obvious biases. The Kruskal–Wallis test was used to compare the three parameters among the BV subsets. In the peripheral CD4, the three subsets were statistically different with respect to the CP frequency ($P < 0.005$), the variance ($P < 0.05$) and the mean CDR3 length ($P < 0.001$). In the CD4 ISP thymocytes, the three BV subsets were not significantly different with respect to the CP frequency and the variance, but significantly different with respect to the CDR3 length ($P < 0.002$). In the CD4 SP and CD8 SP thymocytes, the three BV subsets were different with respect to the CP frequency ($P < 0.05$ for both), the variances ($P < 0.02$ for both) and the mean CDR3 length ($P < 0.001$ and $P < 0.005$ respectively). The three BV subsets from peripheral CD8 were different with respect to the CP frequency ($P < 0.05$), the variance ($P < 0.05$) and the mean CDR3 length ($P < 0.005$). The Mann–Whitney test was used to compare the three parameters of the CD4 ISP thymocytes and the other populations. The CP frequencies of CD4 ISP were always lower than those of CD4 SP in the BV1, 3 and 7 subsets, than those of CD8 SP, than those of peripheral CD4, and than those of peripheral CD8. The variances of CD4 ISP were larger than those of CD4 SP in the BV1 3 and 7 subsets, than those of CD8 SP, than those of peripheral CD4, and than those of peripheral CD8. The mean CDR3 lengths of CD4 ISP were longer than those of CD4 SP, CD8 SP, peripheral CD4, and peripheral CD8 in all three subsets. $^{*}P < 0.05$ and $^{**}P < 0.01$ respectively in the Mann–Whitney test to compare each T cell population with the corresponding CD4 ISP population.

BV1, 3 and 7 subsets ($P < 0.01$ for each subset), than those of CD8 SP ($P < 0.01$, $P < 0.05$, and $P < 0.01$ respectively), than those of peripheral CD4 ($P < 0.01$ for each subset) and than those of peripheral CD8 ($P < 0.01$ for each subset).

As for the mean CDR3 length, the same differences among the three BV subsets were observed in the CD4 and CD8 SP thymocytes, and in the peripheral CD8 T cells (Fig. 3C). Unlike the distribution patterns, the differences in length were already seen in the CD4 ISP thymocytes (Fig. 3C). These results imply that positive and negative selections exert distinct effects on CLS distribution pattern and on CDR3 length.

Cluster analyses segregated the histograms of the CD4 and CD8 SP thymocytes into three groups, each of which contained primarily those of the same BV subset (Fig. 4C and D). The histograms of the peripheral CD8 T cells also fell into the three groups except for the histograms with biases (Fig. 4B). Notably, the same analysis of the histograms of the ISP thymocytes failed to discriminate BV gene use (Fig. 4E). This should be due to similarity of the distribution patterns and suggests that the difference in length alone is not enough for segregation.

BV- and co-receptor-dependent shortening of TCRB CDR3 length in the human thymus

It has been reported that TCR CDR3 shortens during transition from the ISP thymocytes to the SP thymocytes (21). This was observed in our studies of the mean CDR3 length; the CD4 ISP thymocytes had longer CDR3 than the other populations (Fig. 3C). To investigate this further, we analyzed plots of differences in frequency (ΔF) and skew values ($\Sigma\Delta F$), both of which have been defined by Yassai *et al.* (21,22). ΔF can be calculated by subtracting the CLS frequency of a given population from that of the other at the same length. A cluster of positive ΔF values on the right of an inflection point with a corresponding cluster of negative ΔF values on the other side indicates that the given population has shorter CDR3. $\Sigma\Delta F$ is the sum of ΔF values to the right of the inflection points. The ΔF plots and $\Sigma\Delta F$ were calculated by subtraction of the frequencies of the CD4 and CD8 SP thymocytes from those of the CD4 ISP thymocytes in the three BV subsets (Fig. 5A). Their patterns and positive $\Sigma\Delta F$ values showed that both SP thymocyte populations had shorter CDR3 than the CD4 ISP thymocytes irrespective of BV subset.

Interaction of TCR with endogenous antigens dictates CD4/CD8 lineage commitment during positive and negative selections in the thymus. This led us to assume that the shortening could be a function of the lineage if it is a consequence of TCR triggering. We then calculated ΔF between cells with different lineages; between the CD4 and CD8 SP thymocytes and between the peripheral CD4 and CD8 T cells (Fig. 5B). The ΔF plots and $\Sigma\Delta F$ showed that the TCR CDR3 length of CD4 lineage cells was shorter in the BV3 subset, whereas it was longer in the BV7 subset. No significant differences in CDR3 length were seen in the BV1 subset. Thus, differential shortening between CD4 and CD8 lineage cells was observed and it depended on BV gene use.

Additionally, the CD4 SP thymocytes and the peripheral CD4 T lymphocytes, as well as the CD8 SP thymocytes and the peripheral CD8 T lymphocytes, were compared. The results showed that CDR3 of CD4 or CD8 lineage cells do not shorten in the peripheral blood (data not shown).

Discussion

The present study has elucidated how TCR CDR3 length repertoires of CD4 and CD8 T cells in different BV subsets develop in the human thymus and peripheral blood. The CDR3 length repertoires had BV-dependent distribution patterns.

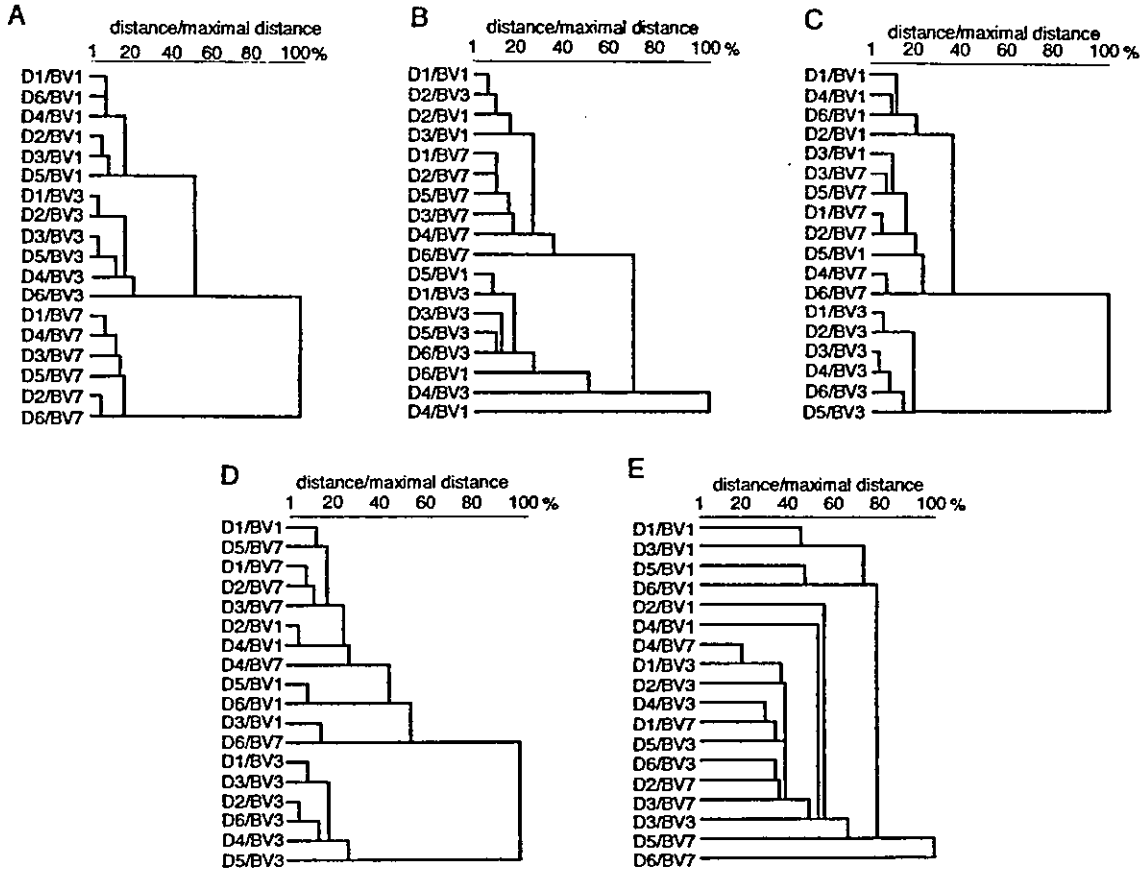

Fig. 4. Cluster analyses of the histograms of individual T cell populations from the six donors. Based on 18 histograms of peripheral CD4 (A) and CD8 (B) T cells, CD4 SP (C) and CD8 SP (D) thymocytes, and CD4 ISP thymocytes (E), the distance of every combination of two histograms was calculated with Ward's method and the Euclidean distance. All calculated distances divided by the maximal distance are shown in a dendrogram. Listed on the left are the BV subsets and the identification of donors that the individual histograms originated from. The BV1 and 3 subsets of the peripheral CD8 T cells from D4 had biased CLS histograms.

They were shaped during thymic selections and maintained in the peripheral blood. In contrast, the BV-dependent differences in the TCR CDR3 length were observed throughout lymphocyte development. The CDR3 became shorter during thymic selections, but did not change the BV-dependent differences seen before the selections. Finally, the degrees of the shortening differed between CD4 and CD8 lineage cells, and also were dependent on BV gene use. The repertoires of peripheral lymphocytes reflected directly those of mature SP thymocytes except for biases induced by clonal expansions.

Although it was known that different CDR3 lengths were preferred by different BV subsets, the BV-dependent distribution patterns are disclosed here for the first time. Unlike the difference in length, the different patterns become evident during positive and negative selections, accompanied by an increase of the CP frequency and narrowing of the distribution span. This argues that they are shaped under the pressure of positive and negative selections in the thymus. Most studies that employed the TCR CLS technique disregarded the differences, probably because the technique was used for identification of gross changes.

We have found that the distribution patterns of three gene members of the BV7 family shared the same characteristics. This ensures that the CLS histograms generated with the primer specific to BV7 family genes were not artifacts. In this regard, we have found that different gene members of the BV6 family could have similar distribution patterns (Fig. 1B). Also, both BV3 and 11 subsets shared histograms with low CP frequencies and large variances. Arden *et al.* (29) pointed out that these two genes are closely related both structurally and in their CDR3 sequences. According to their TCRBV gene classification, BV1, 3 and 7 fall into different groups. These facts argue that the BV-dependent differences could be attributable to the structure of TCRβ chains.

Using murine thymus, Pannetier *et al.* (23) observed that different BV subsets prefer different TCR CDR3 lengths. We found that the BV-dependent difference in mean TCR length already occurred in the CD4 ISP thymocytes. This implies that the difference is regulated by TCR rearrangement. Also, since the CD4 ISP thymocytes with complete TCRB gene rearrangement are under pressure of subsequent β selection for association with pre-Tα chains, the β selection could contribute to the difference formation. Moreover, the CLS histograms

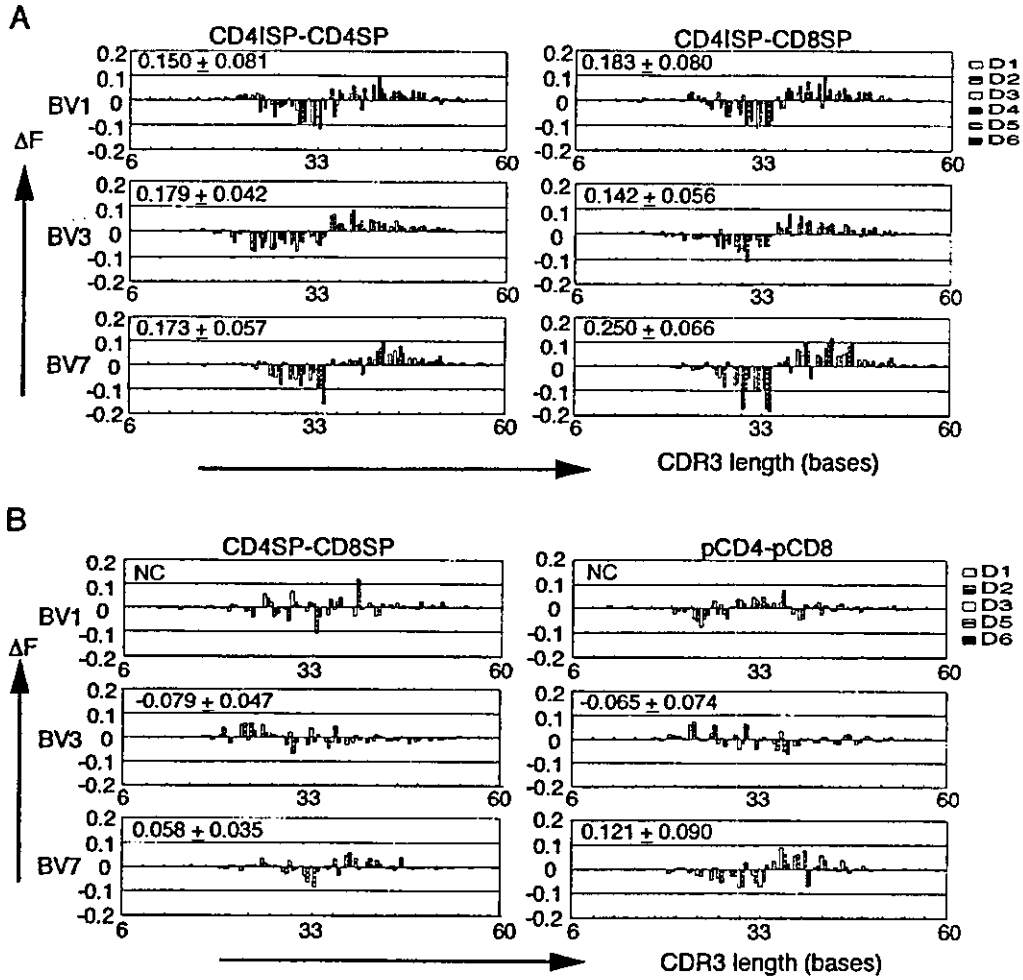

Fig. 5. Comparison of TCR CDR3 length in different CD4/CD8 lineage cells. Plotted are ΔF that were calculated by subtracting the frequencies in the CD4 and CD8 SP thymocytes from those in the ISP thymocytes (A: CD4 ISP – CD4 SP and CD4 ISP – CD8 SP respectively), and by subtracting the frequencies in the CD8 SP thymocytes from those in the CD4 SP thymocytes and those in the peripheral CD8 T cells from those in the peripheral CD4 T cells (B: CD4 SP – CD8 SP and peripheral CD4 – peripheral CD8 respectively). In order to quantify the shortening, the means ± SD of $\Sigma\Delta F$ derived from the six donors were calculated (shown in the panels). In (B), where the data from D4 have been excluded, $\Sigma\Delta F$ values of the BV3 subsets were all negative in both subtractions, while $\Sigma\Delta F$ values of the BV7 subsets were all positive. $\Sigma\Delta F$ values were not calculated for the BV1 subset because no inflection points were found in the ΔF plots. NC, not calculated.

of the BV1, 3 and 7 subsets of the CD4 ISP thymocytes were similar, but not necessarily identical (Fig. 2B), suggesting that the rearrangement and/or β selection may have a subsidiary effect in shaping the CLS distribution patterns.

To address further if the rearrangement *per se* regulates the BV-dependent difference in CDR3 length, we tried to amplify non-productively recombined TCRBV1, 3 and 7 genes from peripheral T lymphocytes that do not express TCRVβ1, 3 or 7. However, even from $>10^7$, a sufficient amount of the rearranged genes could not be amplified for the TCR CLS analyses. This was consistent with the fact that the TCRB CLS patterns of the CD4 ISP thymocytes always had 3-base pair spacing, indicating that all transcripts were in-frame. The 3-base spacing was also observed by Yassai *et al.* (21) who examined TCRB genomic DNA derived from the same population. It is known that 85% of CD4 ISP thymocytes retain the TCRB germline configuration, while only 5% express rearranged TCRB gene products (9). Thus, thymocytes with out-of-frame TCRB rearrangements must be diluted out quickly by those expressing complete TCRβ/pre-Tα and become undetectable with conventional technologies.

In separate experiments, we have assessed the mean TCR CDR3 lengths of the other BV subsets and found that the BV subsets with similar CLS patterns do not necessarily have similar CDR3 length (data not shown). The differences in shortening between CD4 and CD8 lineage cells were not a function of the distribution patterns (data not shown). Thus, distribution pattern and length appeared to be regulated independently.

Yassai *et al.* (21,22) reported TCR shortening in the human and murine thymi. By examining murine thymocytes for the BV1–BJ2 recombinants, they have shown that the shortening

occurs to a larger extent in the CD4 lineage cells than in the CD8 lineage cells. They failed to see differential shortening in humans and suggested a distinct regulation for human thymocytes. However, we observed a clear difference between the CD4 and CD8 T cells. We found that the differential shortening was a function of BV gene use. These data imply that the shortening in humans is regulated by antigen recognition by TCR.

The TCR shortening could be affected by allelic variations of MHC gene products, and differential shortening between CD4 and CD8 lineage cells could be due to differential orthogonal geometry of TCR and antigenic peptide in the grooves of MHC class I and II molecules (22). However, the differences in mean CDR3 length were preserved throughout the thymic selections. The CD4 and CD8 lineage cells share the same CLS distribution patterns. Thus, although limitations in sample collection did not allow us to investigate the effects of HLA variations, the geometry should not be the only factor regulating CDR3 length repertoire.

Development of the TCRB CDR3 length repertoire is regulated delicately in the thymus. Peripheral selections have little effect unless T cell clones expand massively in response to immunological insults. Elucidation of these thymic regulations may shed more light on molecular interaction of TCR with self-peptide–MHC in the thymus.

Acknowledgements

This study was supported by a grant from the Ministry of Health, Labor and Welfare, Japan. The authors thank Dr Takeshi Hiramatsu at Tokyo Women's Medical University for providing us with thymus and peripheral blood samples.

Abbreviations

ΔF	differences in frequency
$\Sigma\Delta F$	skew value
CDR	complementarity-determining region
CLS	CDR3 length spectratyping
CP	central peak
ISP	immature single positive
SP	single positive

References

1 Garboczi, D. N., Ghosh, P., Utz, U., Fan, Q. R., Biddison, W. E. and Wiley, D. C. 1996. Structure of the complex between human T-cell receptor, viral peptide and HLA-A2. *Nature* 384:134.

2 Garcia, K. C., Degano, M., Stanfield, R. L., Brunmark, A., Jackson, M. R., Peterson, P. A., Teyton, L. and Wilson, I. A. 1996. An αβ T cell receptor structure at 2.5 Å and its orientation in the TCR-MHC complex. *Science* 274:209.

3 Jorgensen, J. L., Reay, P. A., Ehrich, E. W. and Davis, M. M. 1992. Molecular components of T-cell recognition. *Annu. Rev. Immunol.* 10:835.

4 Wilson, R. K., Lai, E., Concannon, P., Barth, R. K. and Hood, L. E. 1988. Structure, organization and polymorphism of murine and human T-cell receptor α and β chain gene families. *Immunol. Rev.* 101:149.

5 Davis, M. M. 1990. T cell receptor gene diversity and selection. *Annu. Rev. Biochem.* 59:475.

6 Rammensee, H. G. 1995. Chemistry of peptides associated with *MHC class I and class II molecules. Curr. Opin. Immunol. 7:85.*

7 *Matsushita, S., Takahashi, K., Motoki, M., Komoriya, K., Ikagawa,* S. and Nishimura, Y. 1994. Allele specificity of structural requirement for peptides bound to HLA-DRB1*0405 and -DRB1*0406 complexes: implication for the HLA-associated susceptibility to methimazole-induced insulin autoimmune syndrome. *J. Exp. Med.* 180:873.

8 Ramiro, A. R., Trigueros, C., Marquez, C., San Millan, J. L. and Toribio, M. L. 1996. Regulation of pre-T cell receptor (pTα-TCRβ) gene expression during human thymic development. *J. Exp. Med.* 184:519.

9 Blom, B., Verschuren, M. C., Heemskerk, M. H., Bakker, A. Q., van Gastel-Mol, E. J., Wolvers-Tettero, I. L. M., van Dongen, J. J. M. and Spits, H. 1999. TCR gene rearrangements and expression of the pre-T cell receptor complex during human T-cell differentiation. *Blood* 93:3033.

10 Fehling, H. J., Krotkova, A., Saint-Ruf, C. and von Boehmer, H. 1995. Crucial role of the pre-T-cell receptor α gene in development of αβ but not γδ T cells. *Nature* 375:795.

11 Sebzda, E., Mariathasan, S., Ohteki, T., Jones, R., Bachmann, M. F. and Ohashi, P. S. 1999. Selection of the T cell repertoire. *Annu. Rev. Immunol.* 17:829.

12 Pannetier, C., Even, J. and Kourilsky, P. 1995. T-cell repertoire diversity and clonal expansions in normal and clinical samples. *Immunol. Today* 16:176.

13 Hingorani, R., Choi, I. H., Akolkar, P., Gulwani, A. B., Pergolizzi, R., Silver, J. and Gregersen, P. K. 1993. Clonal predominance of T cell receptors within the CD8+ CD45RO+ subset in normal human subjects. *J. Immunol.* 151:5762.

14 Gorski, J., Yassai, M., Zhu, X., Kissela, B., Keever, C. and Flomenberg, N. 1994. Circulating T cell repertoire complexity in normal individuals and bone marrow recipients analyzed by CDR3 size spectratyping. Correlation with immune status. *J. Immunol.* 152:5109.

15 Schwab, R., Szabo, P., Manavalan, J. S., Weksler, M. E., Posnett, D. N., Pannetier, C., Kourilsky, P. and Even, J. 1997. Expanded CD4+ and CD8+ T cell clones in elderly humans. *J. Immunol.* 158:4493.

16 Maccalli, C., Farina, C., Sensi, M., Parmiani, G. and Anichini, A. 1997. TCR β-chain variable region-driven selection and massive expansion of HLA-class I-restricted antitumor CTL lines from HLA-A*0201+ melanoma patients. *J. Immunol.* 158:5902.

17 Lin, M. Y. and Welsh, R. M. 1998. Stability and diversity of T cell receptor repertoire usage during lymphocytic choriomeningitis virus infection of mice. *J. Exp. Med.* 188:1993.

18 Sourdive, D. J., Murali, K. K., Altman, J. D., Zajac, A. J., Whitmire, J. K., Pannetier, C., Kourilsky, P., Evavold, B., Sette, A. and Ahmed, R. 1998. Conserved T cell receptor repertoire in primary and memory CD8 T cell responses to an acute viral infection. *J. Exp. Med.* 188:71.

19 Nishio, J., Suzuki, M., Miyasaka, N. and Kohsaka, H. 2001. Clonal biases of peripheral CD8 T cell repertoire directly reflect local inflammation in polymyositis. *J. Immunol.* 167:4051.

20 Moss, P. A. and Bell, J. I. 1995. Sequence analysis of the human αβ T-cell receptor CDR3 region. *Immunogenetics* 42:10.

21 Yassai, M. and Gorski, J. 2000. Thymocyte maturation: selection for in-frame TCR α-chain rearrangement is followed by selection for shorter TCR β-chain complementarity-determining region 3. *J. Immunol.* 165:3706.

22 Yassai, M., Ammon, K., Goverman, J., Marrack, P., Naumov, Y. and Gorski, J. 2002. A molecular marker for thymocyte-positive selection: selection of CD4 single-positive thymocytes with shorter TCRB CDR3 during T cell development. *J. Immunol.* 168:3801.

23 Pannetier, C., Cochet, M., Darche, S., Casrouge, A., Zoller, M. and Kourilsky, P. 1993. The sizes of the CDR3 hypervariable regions of the murine T-cell receptor β chains vary as a function of the recombined germ-line segments. *Proc. Natl Acad. Sci. USA* 90:4319.

24 Hall, M. A. and Lanchbury, J. S. 1995. Healthy human T-cell receptor β-chain repertoire. Quantitative analysis and evidence for J β-related effects on CDR3 structure and diversity. *Hum. Immunol.* 43:207.

25 Nanki, T., Kohsaka, H. and Miyasaka, N. 1998. Development of human peripheral TCRBJ gene repertoire. J. Immunol. 161:228.

26 Kohsaka, H., Taniguchi, A., Chen, P. P., Ollier, W. E. R. and

Carson, D. A. 1993. The expressed T cell receptor V gene repertoire of rheumatoid arthritis monozygotic twins:rapid analysis by anchored polymerase chain reaction and enzyme-linked immunosorbent assay. *Eur. J. Immunol.* 23:1895.

27 Callahan, J. E., Kappler, J. W. and Marrack, P. 1993. Unexpected expansions of CD8-bearing cells in old mice. *J. Immunol.* 151:6657.

28 Novak, E. J., Liu, A. W., Nepom, G. T. and Kwok, W. W. 1999. MHC class II tetramers identify peptide-specific human CD4+ T cells proliferating in response to influenza A antigen. *J. Clin. Invest.* 104:R63.

29 Arden, B., Clark, S. P., Kabelitz, D. and Mak, T. W. 1995. Human T-cell receptor variable gene segment families. *Immunogenetics* 42:455.

30 Williams, A. F., Strominger, J. L., Bell, J., Mak, T. W., Kappler, J., Marrack, P., Arden, B., Lefranc, M. P., Hood, L., Tonegawa, S. and Davis, M. 1993. Nomenclature for T-cell receptor (TCR) gene segments of the immune system. *WHO Bull.* 71:113.

Stimulation of Host NKT Cells by Synthetic Glycolipid Regulates Acute Graft-versus-Host Disease by Inducing Th2 Polarization of Donor T Cells[1]

Daigo Hashimoto,* Shoji Asakura,* Sachiko Miyake,† Takashi Yamamura,† Luc Van Kaer,‡ Chen Liu,§ Mitsune Tanimoto,* and Takanori Teshima[2]*¶

NKT cells are a unique immunoregulatory T cell population that produces large amounts of cytokines. We have investigated whether stimulation of host NKT cells could modulate acute graft-vs-host disease (GVHD) in mice. Injection of the synthetic NKT cell ligand α-galactosylceramide (α-GalCer) to recipient mice on day 0 following allogeneic bone marrow transplantation promoted Th2 polarization of donor T cells and a dramatic reduction of serum TNF-α, a critical mediator of GVHD. A single injection of α-GalCer to recipient mice significantly reduced morbidity and mortality of GVHD. However, the same treatment was unable to confer protection against GVHD in NKT cell-deficient CD1d knockout ($CD1d^{-/-}$) or $IL\text{-}4^{-/-}$ recipient mice or when $STAT6^{-/-}$ mice were used as donors, indicating the critical role of host NKT cells, host production of IL-4, and Th2 cytokine responses mediated by donor T cells on the protective effects of α-GalCer against GVHD. Thus, stimulation of host NKT cells through administration of NKT ligand can regulate acute GVHD by inducing Th2 polarization of donor T cells via STAT6-dependent mechanisms and might represent a novel strategy for prevention of acute GVHD. ***The Journal of Immunology*****, 2005, 174: 551–556.**

Allogeneic hemopoietic stem cell transplantation (HSCT)[3] cures various hematologic malignant tumors, bone marrow (BM) failures, and congenital metabolic disorders. Emerging evidence suggests that allogeneic HSCT is also useful for treatment of other diseases, including solid tumors and autoimmune diseases (1, 2). However, graft-vs-host disease (GVHD) is a major obstacle that precludes wider application of allogeneic HSCT. The pathophysiology of acute GVHD is complex, involving 1) donor T cell responses to the host alloantigens expressed by host APCs activated by conditioning regimens (i.e., irradiation and/or chemotherapy), and 2) dysregulation of inflammatory cytokine cascades, leading to further T cell expansion and induction of cytotoxic T cell responses (3).

$CD4^+$ helper T cells can be divided into two distinct subpopulations: Th1 and Th2 cells (4). Th1 cells produce IFN-γ and IL-2, whereas Th2 cells produce IL-4, IL-5, and IL-13. Although the role of Th1 and Th2 cytokines in the pathophysiology of acute GVHD is complex and controversial (5–8), Th1 polarization of donor T cells predominantly plays a role in inducing the "cytokine storm" that is seen in several models of acute GVHD (3, 9), whereas Th2 polarization mostly suppresses inflammatory cascades and reduces acute GVHD (10–12). Many properties of dendritic cells (DCs), including the type of signal, the duration of activation, the ratio of DCs to T cells, and the DC subset that presents the Ag, influence the differentiation of naive $CD4^+$ T cells into Th1 or Th2 cells (13). The cytokines that are present during the initiation of the immune responses at the time when the TCR engages with MHC/peptide Ags are critically important for Th cell differentiation (14).

NKT cells are a distinct subset of lymphocytes characterized by expression of surface markers of NK cells together with a TCR. Although the NKT cell population exhibits considerable heterogeneity with regard to phenotypic characteristics and functions (15), the major subset of murine NKT cells expresses a semi-invariant TCR, Vα14-Jα18, in combination with a highly skewed set of Vβs, mainly Vβ8 (16). NKT cells can be activated via their TCR by glycolipid Ags presented by the nonpolymorphic MHC class I-like molecule CD1d expressed by APCs (17). Stimulation of NKT cells rapidly induces secretion of large amounts of IFN-γ and IL-4, thereby influencing the Th1/Th2 balance of conventional $CD4^+$ T cell responses (18). In particular, NKT cells are considered an important early source of IL-4 for the initiation of Th2 responses (19, 20), although these cells are not absolutely required for the induction of Th2 responses (21–23). NKT cells are absent in CD1d knockout ($CD1d^{-/-}$) mice because of defects in their thymic positive selection, which requires CD1d expression on hemopoietic cells, probably double-positive thymocytes (24, 25).

Considering the critical role of cytokines in the development of acute GVHD, we investigated the role of host NKT cells in an experimental model of GVHD, using synthetic NKT cell ligands,

*Biopathological Science, Okayama University Graduate School of Medicine and Dentistry, Okayama, Japan; †Department of Immunology, National Institute of Neuroscience, Tokyo, Japan; ‡Department of Microbiology and Immunology, Vanderbilt University School of Medicine, Nashville, TN 37232; §Department of Pathology, University of Florida College of Medicine, Gainesville, FL 32610; and ¶Center for Cellular and Molecular Medicine, Kyushu University Hospital, Fukuoka, Japan

Received for publication August 6, 2004. Accepted for publication October 15, 2004.

The costs of publication of this article were defrayed in part by the payment of page charges. This article must therefore be hereby marked *advertisement* in accordance with 18 U.S.C. Section 1734 solely to indicate this fact.

[1] This work was supported by research funds from the Ministry of Education, Culture, Sports, Science and Technology Grant 15591007 (to T.T.), by the Health and Labor Science Research Grants for Clinical Research for Evidence Based Medicine (to T.T.), by grants from the Ministry of Health, Labour, and Welfare of Japan (to T.Y.), by the Organization for Pharmaceutical Safety and Research (to T.Y.), and by a grant-in-aid for cancer research from the Fukuoka Cancer Society.

[2] Address correspondence and reprint requests to Dr. Takanori Teshima, Center for Cellular and Molecular Medicine, Kyushu University Hospital, 3-1-1 Maidashi, Higashi-ku, Fukuoka 812-8582, Japan. E-mail address: tteshima@cancer.med.kyushu-u.ac.jp

[3] Abbreviations used in this paper: HSCT, hemopoietic stem cell transplantation; BM, bone marrow; GVHD, graft-vs-host disease; DC, dendritic cell; α-GalCer, α-galactosylceramide; BMT, bone marrow transplantation; TBI, total body irradiation; TCD, T cell depletion; LN, lymph node; WT, wild type.

0022-1767/05/$02.00

α-galactosylceramide (α-GalCer) (26), a glycolipid originally purified from a marine sponge, and its analog, OCH (27). Our findings indicate that stimulation of host NKT cells with NKT ligands can modulate acute GVHD.

Materials and Methods

Mice

Female C57BL/6 (B6, H-2^b) and BALB/c (H-2^d) mice were purchased from Charles River Japan. IL-4$^{-/-}$ B6 and STAT6$^{-/-}$ BALB/c mice were purchased from The Jackson Laboratory. CD1d$^{-/-}$ B6 mice were established by specific deletion of the CD1d1 gene segment (22). Mice, between 8 and 16 wk of age, were maintained in a specific pathogen-free environment and received normal chow and hyperchlorinated drinking water for the first 3 wk post-bone marrow transplantation (BMT). All experiments involving animals were performed under the auspices of the Institutional Animal Care and Research Advisory Committee at the Department of Animal Resources, Okayama University Advanced Science Research Center.

Bone marrow transplantation

Mice were transplanted according to a standard protocol described previously (28). Briefly, B6 mice received lethal total body irradiation (TBI; x-ray), split into two doses separated by 6.5 h to minimize gastrointestinal toxicity. Recipient mice were injected with 5 × 10^6 BM cells plus 5 × 10^6 spleen cells from either syngeneic (B6) or allogeneic (BALB/c) donors. T cell depletion (TCD) of donor BM cells was performed using anti-CD90 MicroBeads and the AutoMACS system (Miltenyi Biotec) according to the manufacturer's instructions. Donor cells were resuspended in 0.25 ml of HBSS (Invitrogen Life Technologies) and injected i.v. into recipients on day 0. Survival was monitored daily. The degree of systemic acute GVHD was assessed weekly by a scoring system incorporating five clinical parameters: weight loss, posture (hunching), activity, fur texture, and skin integrity, as described (29).

Glycolipids

α-GalCer, (2S,3S,4R)-1-*O*-(α-D-galactopyranosyl)-2-(*N*-hexacosanoylamino)-1,3,4-octadecanetriol (KRN7000), was synthesized and provided by Kirin Brewery Company (30). A homologue of α-GalCer, OCH, was selected from a panel of synthesized α-GalCer analogues by replacing the sugar moiety and/or truncating the aliphatic chains, because of its ability to stimulate enhanced IL-4 and reduced IFN-γ production by NKT cells, as previously described (27, 31). BMT recipient mice were injected i.p. with α-GalCer or OCH (100 μg/kg) immediately after BMT on day 0. Mice from the control groups received the diluent only.

Flow cytometric analysis

mAbs used were FITC- or PE-conjugated anti-mouse CD4, H-2K^b, and H-2K^d (BD Pharmingen). Cells were preincubated with 2.4G2 mAb (rat anti-mouse FcγR) for 10 min at 4°C to block nonspecific binding of labeled Abs, and then were incubated with the relevant mAbs for 15 min on ice. Finally, cells were washed twice with 0.2% BSA in PBS and fixed. After lysis of RBCs with FACS lysing solution (BD Pharmingen), cells were analyzed using a FACSCalibur flow cytometer (BD Biosciences). 7-Amino-actinomycin D (BD Pharmingen)-positive cells (i.e., dead cells) were excluded from the analysis. Fluorochrome-conjugated irrelevant IgG were used as negative controls. At least 5000 live events were acquired for analysis.

Cell cultures

Mesenteric lymph nodes (LNs) and spleens were removed from animals 6 days after BMT and four to six mesenteric LNs or spleens from each experimental group were combined. Numbers of cells were normalized for T cells and were cultured in complete DMEM (Invitrogen Life Technologies) supplemented with 10% FCS, 50 U/ml penicillin, 50 μg/ml streptomycin, 2 mM L-glutamine, 1 mM sodium pyruvate, 0.1 mM nonessential amino acids, 0.02 mM 2-ME, and 10 mM HEPES in wells of a 96-well flat-bottom plate, at a concentration of 5 × 10^4 T cells/well with 1 × 10^5 irradiated (20 Gy) peritoneal cells harvested from naive B6 (allogeneic) animals, or with 5 μg/ml plate-bound anti-CD3ε mAbs (BD Pharmingen) and 2 μg/ml anti-CD28 mAbs (BD Pharmingen). Forty-eight hours after the initiation of culture, supernatants were collected for the measurement of cytokine levels.

ELISA

ELISA was performed according to the manufacturer's protocols (R&D Systems) for measurement of IFN-γ, IL-4, and TNF-α levels, as described previously (32). Samples were obtained from culture supernatant and blood from retro-orbital plexus, diluted appropriately, and run in duplicate. Plates were read at 450 nm using a microplate reader (Bio-Rad). The sensitivity of the assays was 31.25 pg/ml for IFN-γ, 7.6 pg/ml for IL-4, and 23.4 pg/ml for TNF-α.

Histology

Formalin-preserved livers and small and large bowels were embedded in paraffin, cut into 5-μm-thick sections, and stained with H&E for histological examination. Slides were coded without reference to prior treatment and examined in a blinded fashion by a pathologist (C. Liu). A semiquantitative scoring system was used to assess the following abnormalities known to be associated with GVHD, as previously described (33): 0, normal; 0.5, focal and rare; 1.0, focal and mild; 2.0, diffuse and mild; 3.0, diffuse and moderate; and 4.0, diffuse and severe. Scores were added to provide a total score for each specimen. After scoring, the codes were broken and data were compiled. Pathological GVHD scores of intestine are the sum of scores for small bowel and colon.

Statistical analysis

Mann-Whitney *U* test was applied for the analysis of cytokine data and clinical scores. We used the Kaplan-Meier product limit method to obtain survival probability, and the log-rank test was applied for comparing survival curves. Differences in pathological scores between the α-GalCer-treated group and the diluent-treated group were examined by two-way ANOVA. We defined $p < 0.05$ as statistically significant.

Results

Administration of α-GalCer stimulates lethally irradiated mice to produce IFN-γ and IL-4

We first determined whether administration of synthetic NKT ligands such as α-GalCer and OCH can stimulate heavily irradiated mice to produce cytokines. B6 mice were given 13 Gy TBI and were injected i.p. with α-GalCer, OCH, or diluent 2 h after TBI. Six hours later, blood samples were obtained, and serum samples were prepared for measurement of IFN-γ and IL-4. TBI alone or BMT itself did not stimulate diluent-treated mice to produce IFN-γ or IL-4 (Fig. 1). Administration of α-GalCer increased serum levels of IFN-γ and IL-4, even in mice receiving TBI. However, serum levels of IFN-γ were much less in irradiated mice than in unirradiated mice. By contrast, the ability of irradiated mice to produce IL-4 to α-GalCer was maintained for 48 h after irradiation. Serum levels of IFN-γ and IL-4 in response to α-GalCer were not altered when irradiated wild-type (WT) mice were injected with 5 × 10^6 BM cells and 5 × 10^6 spleen cells isolated from allogeneic (BALB/c) donors. Furthermore, these cytokine responses were not observed when α-GalCer was injected into irradiated NKT cell-deficient CD1d$^{-/-}$ mice with or without BMT. These results suggest that host NKT cells that survive for at least 48 h after irradiation, rather than from infused donor cells, are critically involved in the production of these cytokines in response to glycolipids. Irradiation appears to impair the ability of mice to produce IFN-γ while preserving IL-4 production in response to α-GalCer. Similar cytokine profiles were observed when OCH was administered (data not shown).

Administration of α-GalCer to recipients polarizes donor T cells toward Th2 cytokine production after allogeneic BMT

Induction of GVHD fundamentally depends upon donor T cell responses to host alloantigens. We next evaluated the effect of glycolipid administration on donor T cell responses after allogeneic BMT in a well-characterized murine model of acute GVHD (BALB/c→ B6) directed against both MHC and multiple minor histocompatibility Ags. Lethally irradiated B6 mice were transplanted with 5 × 10^6 BM cells and 5 × 10^6 spleen cells from